Neural Coding 2021

14th International Neural Coding Workshop

Seattle, Washington, USA
July 26–29, 2021
Worldwide Online

Schedule of Presentations

All times below are U.S. West Coast/Pacific Daylight Time (PDT) using 24-hour format. Talks are 15 minutes, with 5 minutes for brief questions directly afterwards. We have also reserved 30 minutes for discussions after each group of presentations, during which we will have Zoom breakout rooms for each speaker to meet with colleagues; the main Zoom session will remain open during that time for general discussion. All registered participants will receive Zoom URLs and related information prior to the start of the meeting.

City	Start Time	End Time (Monday)	End Time (Tue/Thu)	End Time (Wednesday)
Seattle	5:00	9:35	9:00	9:30
New York	8:00	12:35	12:00	12:30
Montevideo	9:00	13:35	13:00	13:30
London	13:00	17:35	17:00	17:30
Tokyo	21:00	1:35	1:00	1:30

Monday

Time (PDT)	Paper #	Author(s)	Title
5:00	Welcome		
5:05	20	Tomasz M. Rutkowski, Masato S. Abe, Seiki Tokunaga, Tomasz Komendzinski and Mihoko Otake-Matsuura	Classifying Mild Cognitive Impairment from EEG Patterns for Dementia Onset Prediction
5:25	28	Michael DePass, Ali Falaki, Stephan Quessy, Numa Dancause and Ignasi Cos	A Mesoscopic Characterization of Sequential Movement related Neuro-motor States in Premotor and Motor Cortices: A Machine Learning Approach
5:45	34	Qinyue Zheng, Sihao Liu, Alessandro Villa and Alessandra Lintas	Brain activity associated with personality traits and behavioral strategies revealed by unsupervised analysis of EEG Signal
6:05	Discussion in breakout rooms		
6:35	6	Viacheslav Osaulenko and Danylo Ulianych	Model of cell assemblies formation with iterative winners-take-all computation and excitation–inhibition balance

6:55	12	Rimjhim Tomar and Lubomir Kostal	Instantaneous Firing Rate Dispersion Can Decrease With Increasing Inter-spike Interval Variability
7:15	18	Irene Tubikanec, Massimiliano Tamborrino, Petr Lansky and Evelyn Buckwar	Qualitative properties of numerical methods for the inhomogeneous geometric Brownian motion
7:35	Discussion in breakout rooms		
8:05	21	Charles Smith	Origins and consequences of serial dependence in vestibular neural models
8:25	1	Cesar Ceballos, Rodrigo Pena and Antonio Roque	Impact of the activation rate of the Ih current influences the neuronal membrane time constant and synaptic potential duration
8:45	19	Helena Bordini de Lucas, Steven L. Bressler, Fernanda Selingardi Matias and Osvaldo Anibal Rosso	Using causal information theory to characterize cortical signals during a Go/No-Go task
9:05	Discussion in breakout rooms		
9:35	end		

Tuesday

Time (PDT)	**Paper #**	**Author(s)**	**Title**
5:00	11	Akari Matsuki, Ryota Kobayashi and Hiroshi Kori	Bias in the estimation of coupling strength between oscillators
5:20	32	Takeshi Abe, Yoshiyuki Asai and Alessandro E.P. Villa	Phase coupling in interaction networks of neural mass models of cortical columns
5:40	10	Arun Neru Balachandar, Alexander Khibnik, Joël Tabak and Roman Borisyuk	Duration of the synaptic influence determines phase difference between asymmetrically coupled oscillators
6:00	Discussion in breakout rooms		
6:30	31	Isabella Silkis	Mechanisms of functioning of connectomes each of which includes the neocortex, hippocampus, basal ganglia, cerebellum, and thalamus

6:50	13	Angel Caputi, Alejo Rodiguez-Cattáneo, Ana-Carolina Pereira and Pedro Aguilera	Image processing in a cerebellum like structure
7:10	24	Robin Gutzen, Sonja Grün and Michael Denker	Eigenangles: evaluating the statistical similarity of neural network simulations via eigenvector angles
7:30	Discussion in breakout rooms		
8:00	7	Snigdha Singh, Natalie Gonzales and Michael Stiber	Refining connections in developing neural networks
8:20	27	Lawrence Ward and Priscilla Greenwood	Building stochastic dynamical neural circuits
8:40	Discussion in breakout rooms		
9:00	end		

Wednesday

Time (PDT)	**Paper #**	**Author(s)**	**Title**
5:00	23	Tsai-Rong Chang, Dominik Sorek, Petr Marsalek and Tzai-Wen Chiu	Strong energy component is more important than spectral selectivity in modeling responses of midbrain auditory neurons to wide-band environmental sounds
5:20	25	George Hadjiantonis, Guido Bugmann and Chris Christodoulou	Characterization of inputs from filtered intracellular recordings
5:40	22	Alessandra Stella, Peter Bouss, Günther Palm, Alexa Riehle, Sonja Grün and Thomas Brochier	Significant Spatio-Temporal Spike Patterns in Macaque Monkey Motor Cortex
6:00	Discussion in breakout rooms		
6:30	26	Jacob Kanev, Achilleas Koutsou, Chris Christodoulou and Klaus Obermayer	The Difference Neuron: A versatile abstract spiking neuron model
6:50	33	Alessandra Lintas, Raudel Sánchez-Campusano, Agnes Gruart, José María Delgado-García and Alessandro E.P. Villa	Dynamics of brain activity in multisite recordings from behaving parvalbumin deficient mice (PVKO)
7:10	8	Mauricio Girardi-Schappo, Emilio F. Galera, Tawan T. A. Carvalho, Ludmila Brochini, Nilton L. Kamiji, Antonio C. Roque and Osame Kinouchi	Asynchronous irregular activity coexists with power-law distributed neuronal avalanches
7:30	Discussion in breakout rooms		
8:00	29	Irina Sinakevitch and Wulfila Gronenberg	Olfactory neuropil in Amblypygids

8:20	15	Tomas Barta and Lubomir Kostal	Inhibitory noise decreases membrane potential fluctuations and may lead to increased firing regularity
8:40	35	Henrik Ekström and Tatyana Turova	A non-monotone bootstrap percolation model of neuronal activity
9:00	Discussion in breakout rooms		
9:30	end		

Thursday

Time (PDT)	**Paper #**	**Author(s)**	**Title**
5:00	14	Ryota Kobayashi, Daisuke Endo and Shigeru Shinomoto	Estimating synaptic connectivity from parallel spike trains
5:20	17	Makoto Ozawa, Yasuyuki Suzuki and Taishin Nomura	Gaze-evoked nystagmus with centripetal drifts and centrifugal microsaccades during gaze fixation and its minimal neuromechanical model
5:40	3	Olha Shchur and Alexander Vidybida	Firing statistics of a neuron with delayed feedback inhibition stimulated with a renewal point process
6:00	Discussion in breakout rooms		
6:30	5	Massimiliano Tamborrino and Petr Lansky	Shot noise, weak convergence and diffusion approximations
6:50	9	Petr Lansky, Federico Polito and Laura Sacerdote	Input-output consistency in integrate and fire networks with application to neuronal spiking activity
7:10	16	Marie Levakova and Susanne Ditlevsen	Cointegration analysis of EEG signals
7:30	Discussion in breakout rooms		
8:00	2	Alexander Vidybida, Olha Shchur and Victoria Mochulska	From chaos to clock in reverberating neural net. Case study
8:20	4	Rodrigo Santiago and Adriano Tort	On the boundary conditions of avoidance memory reconsolidation: an attractor network perspective

8:40	Discussion in breakout rooms		
9:00	end		

Index of Presentations

by first author

Impact of the activation rate of the I_h current influences the neuronal membrane time constant and synaptic potential duration*

Cesar C. Ceballos[1], Rodrigo F.O. Pena[2], and Antonio C. Roque[3]

(1) Vollum Institute, Oregon Health & Science University, Portland, OR, USA.

(2) Federated Department of Biological Sciences, New Jersey Institute of Technology and Rutgers University, Newark, New Jersey, NJ, USA.

(3) Department of Physics, School of Philosophy, Sciences and Letters of Ribeirão Preto, University of São Paulo, Ribeirão Preto, SP, Brazil

The hyperpolarization-activated cation current I_h is implicated in a variety of phenomena in neurons, including membrane input resistance, resting potential regulation and synaptic integration. In particular, the I_h current can modulate subthreshold potential changes by shortening excitatory postsynaptic potentials and decreasing their temporal summation [1,2]. The effect of the I_h conductance on synaptic potential shortening is well understood, however the role of the I_h kinetics on the time course of excitatory postsynaptic potentials (EPSPs) is yet unexplained. Here, we use a model of the I_h current model with either fast or slow kinetics to determine its influence on the membrane time constant (τ_m) of a CA1 pyramidal cell model. Our simulation results show that the I_h with fast kinetics decreases τ_m and attenuates and shortens the EPSPs more than the slow I_h. Hence, we conclude that the I_h activation kinetics is able to modulate τ_m and the temporal properties of EPSPs in CA1 pyramidal cells. In order to explain how the I_h kinetics controls τ_m, we propose a new concept called "time scaling factor". We then show that the I_h kinetics influences τ_m by modulating the contribution of the I_h derivative conductance to τ_m. Our results are potentially valid for multiple I_h currents and can help to improve our understanding of the role of the I_h current on neuronal dynamics.

References

[1] M. W. Remme and J. Rinzel. Role of active dendritic conductances in subthreshold input integration. *Journal of computational neuroscience*, *31*(1), 13-30, 2011.

[2] J. C. Magee. Dendritic hyperpolarization-activated currents modify the integrative properties of hippocampal CA1 pyramidal neurons. *Journal of Neuroscience*, *18*(19), 7613-7624, 1998.

* This research was produced as part of the IRTG 1740/TRP 2011/50151-0, funded by the DFG/FAPESP. It was also supported partially by the S. Paulo Research Foundation (FAPESP) Research, Innovation and Dissemination Center for Neuromathematics (CEPID NeuroMat, Grant No. 2013/07699-0). The authors also thank FAPESP support through Grants Nos. 2013/25667-8 (R.F.O.P.), 2015/50122-0 and 2018/20277 (A.C.R.). C.C.C. was supported by a CAPES PhD scholarship. A.C.R. thanks financial support from the National Council of Scientific and Technological Development (CNPq), Grant No. 306251/2014-0. This study was financed in part by the Coordenação de Aperfeiçoamento de Pessoal de Nível Superior-Brasil (CAPES) - Finance Code 001.

From chaos to clock in reverberating neural net. Case study

Alexander Vidybida[1], Olha Shchur[1], Victoria Mochulska[2]
(1) – Bogolyubov Institute for Theoretical Physics, 14-b Metrolohichna str., Kyiv, 03143, Ukraine
(2) – Taras Shevchenko National University of Kyiv, Faculty of Physics, Kyiv, Ukraine

It is now accepted (see, e.g. [1]) that knowing only neuronal types and their interconnections (connectome) is not enough for understanding how a certain type of spatio-temporal activity emerges in the brain. A concept of dynome is proposed as a "collection of experimental and modeling observations" [1], aimed at obtaining a mechanistic explanation of various complex brain dynamics. We believe that complex dynamics is an inherent feature of neural networks with delayed interneuronal communication. A modeling illustration of this feature can be found, e.g. in [2, 3]. In this contribution we propose yet another example of complex dynamical behavior in a simple delayed neural net.

We model numerically a fully connected deterministic network of 25 LIF neurons placed at 5x5 lattice nodes. Propagation delays are taken proportional to the interneuronal distances. The network is initially stimulated with a short sequence of 25 input impulses, each triggering one of the 25 neurons. The sequence of the triggering moments constitutes a stimulus specificity. After the initial stimulation, the network runs on its own, without external influence. A stimulus has been found which triggers a seemingly chaotic behavior of the network's state parameters, such as voltage of a neuron. This type of dynamics lasts for a long time ($T_r = 7.3$ minutes) as compared to the lattice diagonal propagation delay, $T_d = 5.7$ milliseconds. After that, the dynamics becomes periodic with period $T_p = 9.6$ milliseconds. The relaxation dynamics is positively checked for being chaotic by several standard tests such as 0-1 test, arithmetic entropy, and sensitivity to small perturbations of the input stimulus.

References

[1] N. J. Kopell, H. J. Gritton, M. A. Whittington, and M. A. Kramer. Beyond the connectome: The dynome. *Neuron*, 83(6):1319–1328, 2014.

[2] A. K. Vidybida. Testing of information condensation in a model reverberating spiking neural network. *International Journal of Neural Systems*, 21(3):187–198, 2011.

[3] A. Vidybida and O. Shchur. Information reduction in a reverberatory neuronal network through convergence to complex oscillatory firing patterns. *BioSystems*, 161:24–30, 2017.

Firing statistics of a neuron with delayed feedback inhibition stimulated with a renewal point process

Olha Shchur[1] and Alexander Vidybida[1]

(1) – Bogolyubov Institute for Theoretical Physics, 14-b Metrolohichna str. Kyiv, 03143, Ukraine

Recently, the importance of cortical disinhibition – the transient ceasing of inhibition – was recognized for various functions, for instance, learning and memory [1]. It was shown that for parvalbumin-expressing interneurons the main source of inhibition is autaptic transmission [2]. The latter means that such neurons send synaptic connections not only to other cells but also to themselves. We study the impact of inhibitory autapse on neuronal activity. We consider a class of non-adaptive spiking neuron models with delayed feedback inhibition. The neuron is stimulated with a series of excitatory impulses, representing a stochastic point renewal process. We calculate exactly the probability density function (PDF) $p(t)$ for the distribution of output interspike intervals (ISIs). The calculation is based on the known PDF $p^0(t)$ for the same neuron without feedback and the PDF of ISIs for the input stream $p^{in}(t)$. Obtained results are applied to the case of a neuron with threshold 2 when the time intervals between input impulses are distributed according to the Erlang distribution.

References

[1] J. J. Letzkus, S. B. Wolff, and A. Lüthi. Disinhibition, a Circuit Mechanism for Associative Learning and Memory. *Neuron*, 88(2):264–276, 2015.

[2] C. Deleuze, G. S. Bhumbra, A. Pazienti, J. Lourenço, C. Mailhes, A. Aguirre, M. Beato, and A. Bacci. Strong preference for autaptic self-connectivity of neocortical PV interneurons facilitates their tuning to γ-oscillations. *PLOS Biology*, 17(9):e3000419, 2019.

On the boundary conditions of avoidance memory reconsolidation: an attractor network perspective

Rodrigo Santiago and Adriano Tort

Computational Neurophysiology Lab, Brain Institute, Federal University of Rio Grande do Norte, Natal, Brazil

The reconsolidation and extinction of aversive memories and their boundary conditions have been extensively studied. Knowing their network mechanisms may lead to the development of better strategies for the treatment of fear and anxiety related disorders. In 2011, Osan et al. developed a computational model for exploring such phenomena based on attractor dynamics, Hebbian plasticity and synaptic degradation induced by prediction error. This model was able to explain, in a single formalism, experimental findings regarding the freezing behavior of rodents submitted to contextual fear conditioning. In 2017, Radiske et al. showed, in rats subjected to inhibitory avoidance (IA), that the previous knowledge of the current aversive context as non-aversive is a boundary condition for the reconsolidation of the shock memory experienced in that context. In the present work, by adapting the Osan et al. (2011) model to simulate the experimental protocols of Radiske et al. (2017), we show that such boundary condition is compatible with the dynamics of an attractor network that supports a synaptic labilization common to reconsolidation and extinction. Additionally, by varying parameters such as the levels of protein synthesis and degradation, we estimate boundary conditions and predict behavioral outcomes in the IA paradigm that can be tested experimentally.

Funding

This work was supported by CNPq and CAPES (Finance Code 001), Brazil.

References

Osan, R., Tort, A. B. L., & Amaral, O. B. (2011). A mismatch-based model for memory reconsolidation and extinction in attractor networks. *PLOS One*, *6*, e23113.

Radiske, A., Gonzalez, M. C., Conde-Ocazionez, S. A., Feitosa, A., Köhler, C. A., Bevilaqua, L. R., et al. (2017). Prior learning of relevant nonaversive information is a boundary condition for avoidance memory reconsolidation in the rat hippocampus. *Journal of Neuroscience*, *37*, 9675–9685.

Shot noise, weak convergence and diffusion approximations*

Massimiliano Tamborrino [1] and Petr Lansky
(1) – Department of Statistics, University of Warwick

Suppose that events (e.g., jumps representing the excitatory inputs impinging on a neuron) occur in accordance to a Poisson process $N(t)$ with constant rate $\lambda > 0$. Associated with the ith event is a nonnegative random variable J_i, which quantifies the event (e.g., its amplitude). Denote by τ_i the time of the ith event. Consider the stochastic process $X(t)$ given by [**?**]

$$X(t) = \sum_{i=1}^{N(t)} J_i e^{-\alpha(t-\tau_i)}, \qquad X(0) = x_0$$

where $\alpha > 0$ is a constant determining the exponential decay rate. When the J_i are independent and identically distributed random variables, independent of the Poisson process $N(t)$, the process $\{X(t), t \geq 0\}$ is called *shot noise process*.

Here, we consider nonnegative shot noise processes and prove their weak convergence (under suitable derived conditions) to Lévy-driven Ornstein–Uhlenbeck (OU) process, whose features depend on the underlying jump distributions. Among others, we obtain the OU-Gamma and OU-Inverse Gaussian processes, having gamma and inverse gaussian processes as background Lévy processes, respectively. Then, we derive the necessary conditions guaranteeing the diffusion limit to a Gaussian OU process, show that they are not met unless allowing for negative jumps happening with probability going to zero, and quantify the error occurred when replacing the shot noise with the OU process and the non-Gaussian OU processes. The results offer a new class of models to be used instead of the commonly applied Gaussian OU processes to approximate synaptic input currents, membrane voltages or conductances modelled by shot noise in single neuron modelling.

References

[1] M. Tamborrino, P. Lansky. Shot noise, weak convergence and diffusion approximations. *Physica D*, 418, 132845, 2021.

*Funding or other acknowledgment.

Model of cell assemblies formation with iterative winners-take-all computation and excitation–inhibition balance

Viacheslav Osaulenko[1,2] and Danylo Ulianych[2]
(1) – Igor Sikorsky Kyiv Polytechnic Institute, Kyiv, Ukraine
(2) – KyivAIGroup, Kyiv, Ukraine

Cell assembly is a group of repeatedly active interconnected neurons and could be the main candidate to represent and compute information in the brain. Here we present a model of cell assemblies formation that is on a higher abstraction level than spiking neural networks (SNN) but lower than the computation with assemblies [4, 5].

Spiking neural networks express rich and complex spatio-temporal dynamics but it is extremely difficult to link the neural activation and synaptic plasticity with computation and information processing. Computation with assemblies simplifies dynamics and allows to rigorously analyze the association memory [3] and pattern completion. The most common approach to encode information to assembly is a k-winners-take-all function from the random projection of the input [1]. It abstracts away inhibitory neurons and represents information as a vector with k ones, (most active cells). Making the parameter k constant does not allow to encode different input vectors with a variable number of active neurons as observed in biological neural networks. Moreover, a significant amount of evidence shows that inhibitory neurons do not only select the top winners, but also shape excitatory population activity from contextual and top-down inputs [2].

We show that explicit inhibition that balances excitation is necessary to perform such computations as decorrelation, clustering, and habituation. The formation of assemblies with two interacting populations requires an iterative procedure that we call iterative winners-take-all (iWTA). Similar to latency coding, it starts by activating the most active neurons in excitatory and inhibitory populations that provide lateral feedback to both populations as shown in fig.1A. On the next iteration, the neural activation threshold decreases, and new neurons are selected. The iterative procedure continues until excitation and inhibition are mutually balanced. The resulting inhibitory and excitatory cell assemblies are formed from active neurons at each iteration. Fig. 2B illustrates the iWTA for one population where new encoding neurons are shown in green, the resulting cell assembly - in red, and previously active neurons - in black.

Experiments with random input vectors and weights from the Bernoulli distribution show that both populations converge to stable representations. The activation sparsity (fraction of the number of active neurons) depends on the parameters of distribution allowing different input vectors to be encoded with a variable number of active neurons, unlike the common kWTA. One of the main features of kWTA is similarity preservation, that is similar inputs are encoded into similar outputs. We show that iWTA also preserves similarity. However, iWTA does so with more parameters (lateral weights) and more iterations to encode the input. We argue that more parameters are necessary to get richer computations. We show that Hebbian-like

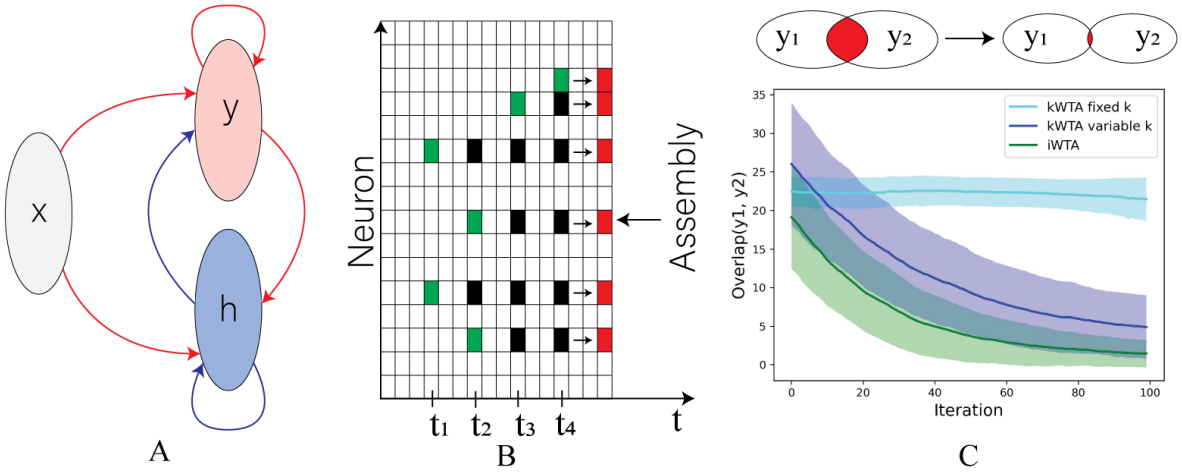

Figure 1: A) the architecture of the network. Layer x is the input, y - excitatory, h - inhibitory populations. B) Schematic illustration of iterative winners-take-all procedure. Each iteration activates new neurons (green). In red shown the output encoding. C) The change of the overlap between two excitatory populations that encode two different inputs with a learning iteration. Learning decorrelates the assemblies while the kWTA activations do not.

learning of inhibitory-excitatory connections reduces the number of active neurons for repeated inputs (habituation). Furthermore, learning these connections decorrelates the encodings of two different inputs, fig.1C. Learning of excitatory-excitatory connections has an opposite effect, the resulting encodings increase their overlap. This overlap encodes the mean pattern from both inputs that can be linked to clustering or noise reduction, but more experiments are required.

Overall, we present a model with explicit inhibitory neurons that through balanced excitation-inhibition and iterative winners-take-all procedure forms neural cell assemblies. The model preserves the advantages of common kWTA but requires more parameters to get richer computations. We hypothesize that learning lateral weights might provide the basic mechanisms for set operations on neural populations.

References

[1] S. Dasgupta, C. F. Stevens, and S. Navlakha. A neural algorithm for a fundamental computing problem. *Science*, 358(6364):793–796, 2017.

[2] J. S. Isaacson and M. Scanziani. How inhibition shapes cortical activity. *Neuron*, 72(2):231–243, 2011.

[3] A. Knoblauch, G. Palm, and F. T. Sommer. Memory capacities for synaptic and structural plasticity. *Neural Computation*, 22(2):289–341, 2010.

[4] G. Palm, A. Knoblauch, F. Hauser, and A. Schüz. Cell assemblies in the cerebral cortex. *Biological cybernetics*, 108(5):559–572, 2014.

[5] C. H. Papadimitriou, S. S. Vempala, D. Mitropolsky, M. Collins, and W. Maass. Brain computation by assemblies of neurons. *Proceedings of the National Academy of Sciences*, 117(25):14464–14472, 2020.

Refining connections in developing neural networks

Snigdha Singh, Natalie Gonzales, Michael Stiber
Computing and Software Systems Division, School of STEM
University of Washington, Bothell, WA 98011, USA

The phases of neural development include genesis of neurons, outgrowth of axons and dendrites to form network connections, and refinement of the network by adjusting and removing synaptic connections [1]. Spike-time-dependent plasticity (STDP) has emerged as one of the most widely used plasticity mechanisms for refinement of neural networks due to its physiological realistic induction and evidence of its presence in vivo [3]. Studying refinement in neural cultures has obvious physiological barriers which prevent collection of detailed information. The current work attempted to develop a better understanding of the biological processes involved in the refinement of the human nervous system by using a neural network simulator to replicate the refinement phase, and record temporal and spatial resolution of individual neuron spiking activity. We present results from simulations implementing STDP to refine a cortical growth neural network model (equivalent to 28 days development in vitro [2]), that demonstrate that network connections get pruned and tuned after STDP, and the process replicates the refinement phase of neural development.

References

[1] B. Alberts, D. Bray, J. Lewis, M. Raff, K. Roberts, and J. Watson. *Molecular Biology of the Cell*. Garland, 4th edition, 2002.

[2] F. Kawasaki and M. Stiber. A simple model of cortical culture growth: burst property dependence on network composition and activity. *Biol Cybern*, 108(4):423–443, Aug. 2014.

[3] S. Song, K. D. Miller, and L. F. Abbott. Competitive Hebbian learning through spike-timing-dependent synaptic plasticity. *Nature Neuroscience*, 3(9):919–926, Sept. 2000. Number: 9 Publisher: Nature Publishing Group.

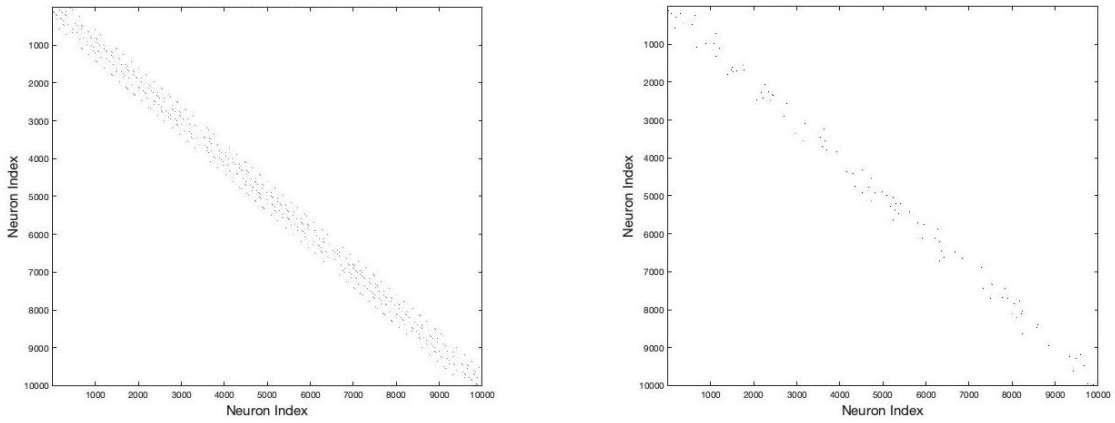

(a) (b)

Figure 1: Edge distribution in the network at the end of the growth simulation and after the STDP simulation. X and Y axes are neuron indices for all 10,000 simulated neurons. Points plotted indicate connections between neurons. Limited resolution in this graph precludes presentation of the full detail of the 10,000 by 10,000 connection matrix. After growth, the network has a recurring pattern, indicating uniform symmetric connections due to repetition in the network layout (a). After STDP, the network has asymmetric connections and significantly less number of points (connections) than in the growth network (b). This reflects the decreased number of connections after pruning using STDP.

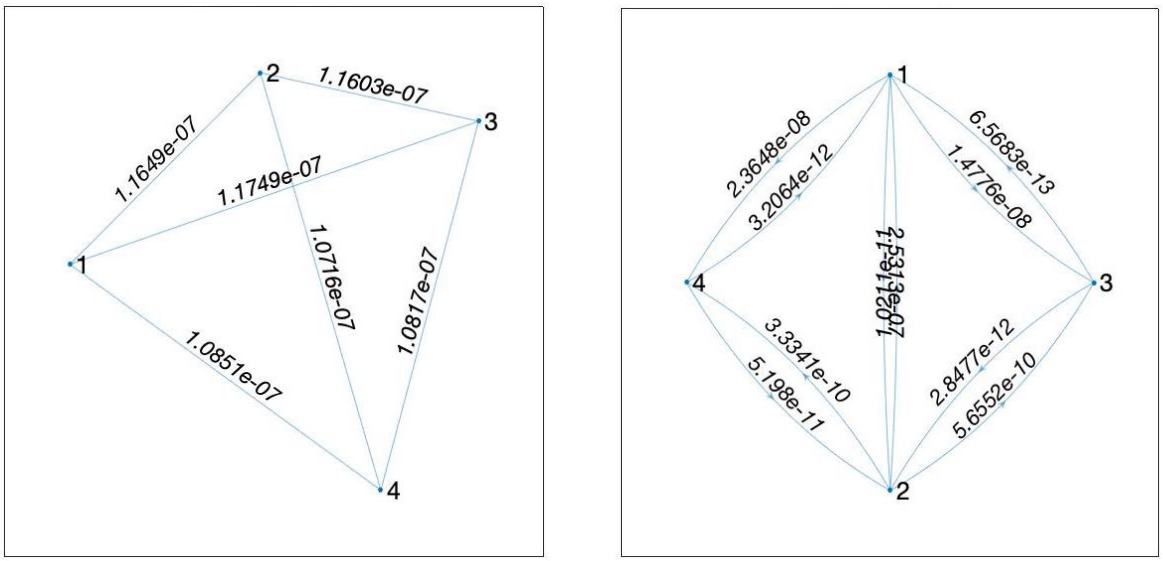

(a) (b)

Figure 2: Change in connections between four central nodes at the end of the growth simulation and after the STDP simulation. Points denote nodes and lines connecting them represent edges. At the end of the growth simulation, edges are bidirectional (a). After STDP, edges are unidirectional as weights get strengthened in one direction and weakened in the other, the connection between nodes 4 to 3 is pruned, and all other synaptic weights are tuned (b).

Asynchronous irregular activity coexists with power-law distributed neuronal avalanches*

Mauricio Girardi-Schappo[1*], Emilio F. Galera[2], Tawan T. A. Carvalho[3], Ludmila Brochini[4], Nilton L. Kamiji[2], Antonio C. Roque[2], Osame Kinouchi[2]

(1) Department of Physics, University of Ottawa, Ottawa, ON, K1N 6N5, Canada

(2) Departamento de Física, FFCLRP, Universidade de São Paulo, Ribeirão Preto, SP, 14040-901, Brazil

(3) Departamento de Física, Universidade Federal de Pernambuco, Recife, PE, 50670-901, Brazil

(4) Instituto de Matemática e Estatística, Universidade de São Paulo, São Paulo, SP, 05508-090, Brazil

Neuronal avalanches and asynchronous irregular (AI) firing patterns have been thought to represent distinct frameworks to understand the brain spontaneous activity. While neuronal avalanches are typically found in systems with slow accumulation and fast dissipation of tension, AI activity happens due to a fluctuation-driven state due to excitation and inhibition (E/I) synaptic balance. Here, we develop a new theory of E/I balance that relies on two homeostatic adaptation mechanisms: the short-term depression of inhibition and the spike-dependent threshold increase, both of which are biological mechanisms [1, 2]. In an early work, we numerically showed that these two mechanisms are capable of generating synaptic balance with AI activity via the mechanism of Self-Organized quasicriticality [3].

However, the relation between SOqC, AI firing via synaptic balance and power-law (PL) distributed neuronal avalanches is not entirely known. While some authors advocate that AI is incompatible with PL avalanches [4], others showed that these two regimes are separated in the phase diagram of a particular model [5]. Here, we develop an analytical theory supported by computational simulations of neuronal networks and show that these two regimes (AI and PL avalanches due to SOqC) happen simultaneously. And more interestingly, such coexistence always happens under self-organized synaptic balance, irrespective of any fine-tuned model parameter [6].

First, we turn off the adaptation and show that the thus defined static system has a typical critical point commonly attributed to self-organized critical models [7]. Then, we turn on the adaptation and show that the network evolves to a dynamic regime in which: (I) E/I synapses balance regardless of any parameter choice; (II) an AI firing pattern emerges; and (III) neuronal avalanches display power laws. This is the first time that these three phenomena appear simultaneously in the same network activity. Thus, we show that the apparently opposing frameworks are unified into a single dynamics thanks to the adaptation mechanisms. In our model, the AI firing pattern is a direct consequence of the hovering close to the critical line where external inputs are compensated by threshold growth, creating synaptic balance for any E/I weight ratio.

*This article was produced as part of the S. Paulo Research Foundation (FAPESP) Research, Innovation and Dissemination Center for Neuromathematics (CEPID NeuroMat, Grant No. 2013/07699-0). The authors also thank FAPESP support through Grants No. 2015/50122-0 (A.C.R.), 2016/03855-5 (N.L.K.), 2016/24676-1 (L.B.), 2018/09150-9 (M.G.-S.), 2018/20277-0 (A.C.R.), and 2019/12746-3 (O.K). A.C.R. thanks the financial support from the National Council of Scientific and Technological Development (CNPq), Grant No. 306251/2014-0. O.K. thanks the Center for Natural and Artificial Information Processing Systems (CNAIPS)-USP. M.G.-S. thanks the financial support of NSERC grant BCPIR/493076-2017 from A. Longtin and L. Maler.

References

[1] S. Denève and C. K. Machens. Efficient codes and balanced networks. *Nat. Neurosci.*, 19:375–382, 2016.

[2] C. Teeter, R. Iyer, V. Menon, N. Gouwens, D. Feng, J. Berg, A. Szafer, N. Cain, H. Zeng, M. Hawrylycz, C. Koch, and S. Mihalas. Generalized leaky integrate-and-fire models classify multiple neuron types. *Nat. Comm.*, 9:709, 2018.

[3] M. Girardi-Schappo, L. Brochini, A. A. Costa, T. T. A. Carvalho, and O. Kinouchi. Synaptic balance due to homeostatically self-organized quasicritical dynamics. *Phys. Rev. Research*, 2:012042(R), 2020.

[4] J. Touboul and A. Destexhe. Power-law statistics and universal scaling in the absence of criticality. *Phys. Rev. E*, 95:012413, 2017.

[5] J. Li and W. L. Shew. Tuning network dynamics from criticality to an asynchronous state. *PLOS Comput. Biol.*, 16:1–16, 2020.

[6] M. Girardi-Schappo, E. F. Galera, T. T. A. Carvalho, L. Brochini, N. L. Kamiji, A. C. Roque, and O. Kinouchi. A unified theory of E/I synaptic balance, quasicritical neuronal avalanches and asynchronous irregular spiking. *bioRxiv*, page 423201, 2020.

[7] T. T. A. Carvalho, A. J. Fontenele, M. Girardi-Schappo, T. Feliciano, L. A. A. Aguiar, T. P. L. Silva, N. A. P. de Vasconcelos, P. V. Carelli, and M. Copelli. Subsampled directed-percolation models explain scaling relations experimentally observed in the brain. *Front. Neural Circuits*, 14:576727, 2021.

Input-output consistency in integrate and fire networks with application to neuronal spiking activity

Petr Lansky[1], **Federico Polito**[2] and Laura Sacerdote[2]

(1) – Institute of Physiology, Academy of Sciences of the Czech Republic, Praha, Czech Republic
(2) – Dipartimento di Matematica, Università di Torino, Italy

Biophysical and more abstract, mathematical, models of neurons aim to describe the information transmission within a neural network. The models are intrinsically stochastic for at least two reasons. First, the experimentally observed neuronal activity is up to a certain extent always characterized by random fluctuations, and secondly stochastic modeling serves as a tool to quantify the information contained in the neuronal activity.
To investigate the information transfer, the input and output part of the network model has to be specified. Up to our knowledge, the consistency between the input network properties and neuronal output has never been investigated. The question posed in this talk is to recognize peculiar properties for which the input to the neurons determines the same properties in the output. In particular, we refer to the distributional properties of input and output ISIs. We will see that the simplicity of the question does not imply a simple answer.
The input-output consistency of network models seems to be connected to the probabilistic concept of "heavy tails" in ISIs distribution. In 1964, Gernstein and Mandelbrot proposed the integrate-and-fire model to account for the observed heavy-tailed behavior of the ISIs distribution. They suggested to modeling the membrane potential through a Wiener process in order to get the inverse Gaussian distribution as its first passage time distribution (i.e. a stable distribution, hence exhibiting heavy tails).
Many alternative and more realistic variants of the original model appeared in the literature in the following decades but the problem of input-output consistency has never been very much considered.
Taking advantage of the recent mathematical progresses on multivariate regularly varying random variables, we propose to formulate the model starting from its main property, i.e. the heavy tails of the ISIs distribution. Then, we follow the integrate-and-fire paradigm to modeling the membrane potential evolution as a randomized random walk whose jumps result from the superposition of the regularly varying inter-times of the post-synaptic signals of the input neurons participating the network. We finally show that input-output consistency is obtained from closure properties of multivariate regularly varying distributions.

References

[1] Gerstein-Mandelbrot "*Random walk models for the spike activity of a single neuron*", Biophys. J. 4, 1964

[2] Lindner "*Superposition of many independent spike trains is generally not a Poisson*

process", PRE 72, 2006

[3] Sacerdote-Giraudo "*Stochastic Integrate and Fire Models*", Stoch. Biom. Mod., 2012

[4] Bingham-Goldie-Teugels "*Regular Variation*", CUP 1987 (2013)

[5] Jessen-Mikosch "*Regularly Varying Functions*", Publ. Inst. Mathématique 79(93), 2006

[6] Resnick *"Heavy-Tail Phenomena: Probabilistic and Statistical Modeling",* Springer, 2007

Duration of the synaptic influence determines phase difference between asymmetrically coupled oscillators*

Arun Neru Balachandar[1], Alexander Khibnik[2] , Joël Tabak[1], Roman Borisyuk[1]

[1]University of Exeter, Exeter, UK
[2]Independent Scientist, Boston, USA

It is critical for animals to have the capability to adjust their locomotor pattern to suit internal and environmental demands, to allow them to move forwards and backwards, to swim in water, fly in air and walk/run/crawl on land. However, the neuronal mechanisms underlying the transitions between motor patterns are poorly understood. A simple experimental animal to examine these questions is the 2-day old hatchling *Xenopus* tadpole, which can swim or struggle [1]. During swimming, a wave of neuronal activity propagates from head to tail, which is reversed during struggling. The spinal cord circuits that generate these activities are well defined, and the mechanisms through which these circuits generate a swimming pattern of activity are well understood. However, current understanding of backward wave propagation and of the transition between the forward and backward patterns is limited [2]. To study possible switching mechanisms, we model the tadpole spinal cord by a chain of identical Morris-Lecar [3] oscillators with directed head-to-tail synaptic coupling (Fig. 1a). We found that this fixed direction of connectivity between identical oscillators can support different directions of activity propagation, depending on the duration of the synaptic influence.

Specifically, with this descending (head-to-tail) excitatory connectivity between oscillators, short synaptic pulses result in a tail to head propagation of activity. However, lengthening influence duration can decrease the phase difference between neighboring oscillators and in some cases reverse it. Thus, studying the chain model, we find that the model parameter ***r***, describing the duration of synaptic influence *relative to the duration of the active phase of the oscillation*, controls the direction of activity propagation (Fig. 1b-c). For a small ***r***, activity propagates backward from tail to head, and in the opposite direction for large ***r***.

To examine how this reversal of the phase difference happens, we focus on two identical relaxation oscillators with a one-way excitatory connection. This reduced model represents the first section of the chain where the most rostral oscillator is the independent driver connected to a driven oscillator. Generally speaking we can expect that the driver generates a spike which forces the driven oscillator to generate a spike with a short phase-delay and this sequence of events will be periodically repeated. However, the limit cycle corresponding to the phase-delay dynamics is unstable.

We find that for a short relative synaptic influence ***r***, there is a stable limit cycle with the phase-advance dynamics: the driven oscillator generates a spike and shortly after the driver spikes (Fig. 2a). This contra-intuitive phase advance phenomena corresponds to the phase advanced limit cycle (A-cycle). Increasing the value of parameter ***r*** leads to a smooth transition to a new phase relationship where a spike of the driven oscillator is preceded with a short delay by a spike of the driver oscillator (Fig. 2b). This phase relationship corresponds to the phase delayed limit cycle (D-cycle). During this transition phase difference (phase of the driven oscillator minus phase of the driver) continuously changes from positive to negative values while the limit cycle remains stable (no bifurcations occur). Fig. 2c shows the phase difference diagram under variation of two model parameters: the relative duration of synaptic influence ***r*** (horizontal axis) and the strength of synaptic influence ***g*** (vertical axis). Color codding

* We would like to acknowledge support from BBSRC UK grants: BB/T002352/1 (RB) and BB/T002549/1 (JT)

shows the phase difference between two oscillators: positive values (brown-green) correspond to A-cycle and negative values (blue) correspond to D-cycle.

We find that the phase-advanced and phase-delayed limit cycles also exist in the Hodgkin-Huxley asymmetrically coupled system and the variation of synaptic duration can switch the sign of phase difference. For asymmetrically coupled Morris-Lecar oscillators both phase relationships exist across a wide range of time-scale-separations and values of external current. Small differences in frequencies of coupled oscillators don't destroy A-cycle, but making the driving oscillator run faster than the driven oscillator will eventually change A-cycle to D-cycle (this transition isn't smooth and involves bifurcations). The effect of the duration of the synaptic influence on the phase difference between the oscillators is also preserved in the presence of a weak coupling from the driven to the driver.

For calculation of the phase difference diagram we combined three techniques: finding limit cycle by solving a periodic boundary value problem, simple continuation using coupling strength as an active parameter, and starting continuation (for given coupling duration) from very low values of coupling strength where limit cycles were calculated semi-analytically as stable fixed points of phase equations derived using Malkin's theorem [4]; deriving phase equations involves computation of iPRC and phase response function for which we use similar approach to [5].

Our results show that a variation in the relative synaptic duration can robustly change the direction of the phase relationship between asymmetrically coupled phase-locked oscillators.

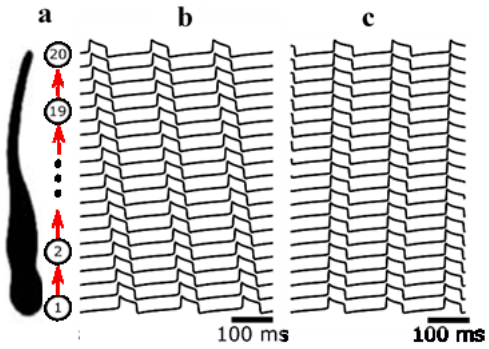

Figure 1. Wave propagation along the chain of Morris-Lecar oscillators.
a. Chain of 20 oscillators with one-way excitatory synaptic connections; direction from 1 to 20 corresponds to rostral-caudal axis in the tadpole spinal cord.
b. From tail to head wave propagation for a small value of parameter ***r***.
c. Rostro-caudal (from head to tail) wave propagation for a large enough value of parameter ***r***.

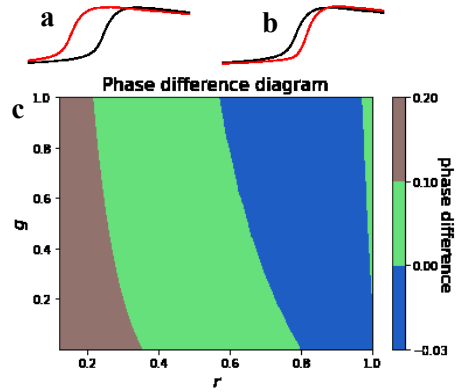

Figure 2. Waveforms of A-cycle and D-cycle and phase difference diagram showing transition between these types.
a-b. Trajectories of A-cycle (left) and D-cycle. Black and red trajectories correspond to the driver and driven oscillators, respectively.
c. Diagram shows the phase difference between two oscillators as a function of two parameters: ***r*** and ***g***.

References

[1] Roberts, A., Li, W. C., & Soffe, S. R. (2010). How neurons generate behaviour in a hatchling amphibian tadpole: an outline. *Frontiers in behavioral neuroscience*, *4*, 16.

[2] Li, W. C., Sautois, B., Roberts, A., & Soffe, S. R. (2007). Reconfiguration of a vertebrate motor network: specific neuron recruitment and context-dependent synaptic plasticity. Journal of Neuroscience, 27(45), 12267-12276. Springer Science & Business Media.

[3] Rinzel, J., & Ermentrout, G. B. (1998). Analysis of neural excitability and oscillations. Methods in neuronal modeling, 2, 251-292.

[4] Hoppensteadt, F. C., & Izhikevich, E. M. (2012). Weakly connected neural networks (Vol. 126).

[5] Ermentrout, B. (1996). Type I membranes, phase resetting curves, and synchrony. Neural computation, 8(5), 979-1001.

Bias in the estimation of coupling strength between oscillators

Akari Matsuki[1], Ryota Kobayashi[2,3,4], and Hiroshi Kori[1,2]
(1) – Graduate School of Information Science and Technology, the University of Tokyo.
(2) – Graduate School of Frontier Sciences, the University of Tokyo.
(3) – MI Center, the University of Tokyo.
(4) – JST PRESTO.

Identification of coupling strength between interacting oscillators from time-series data is an important task [1, 2, 3]. It is known that phase oscillator models well approximate dynamics of weakly coupled oscillators [4]. Once the oscillator phases are extracted somehow from time-series data, one may fit the data to a given phase oscillator model using, e.g., a maximum likelihood estimation. To obtain phases from time-series data, Hilbert transform is often used [5]. However, the estimation of oscillation phases using the Hilbert transform is accurate only in a limited situation. Therefore, in general cases, inferred parameter values using the estimated phases also lack reliability.

We numerically generated oscillatory data of a coupled-oscillators system, obtained the phases using the Hilbert transform, and then estimated the coupling strength. The numerical experiments revealed that the estimation of the coupling strengths is biased when the oscillators are synchronized. The estimated value is roughly half of the true value (Fig. 1). In contrast, the coupling strengths are correctly estimated when the oscillators are not synchronized. Such a property of the Hilbert transform is problematic, for example, in estimating the direction and the network structure of coupling, for which the methods have been discussed [3, 6].

To identify the reason for this property, we analyzed the nature of phase acquisition by the Hilbert transform and found that the high-frequency components of the phase are halved when the Hilbert transform is performed. In other words, the Hilbert transform has the effect of smoothing the phase time series. Therefore, it cannot recover the noisy phase time series correctly. When the oscillators are synchronized, the phase difference between them is fixed around a constant value. In this case, the coupling term represents the response to the change in phase difference mainly caused by noise. Thus, the smoothing effect of the Hilbert transform has a significant effect on the estimation of coupling strength. On the other hand, in the non-synchronized system, the coupling term is the response mainly to the drifting phase difference, and the contribution of noise is relatively small. Thus, the coupling strength is correctly estimated. We have developed a new phase acquisition method based on the analytical results of the Hilbert transform. By using this method, we can accurately recover the noisy phase time series. Furthermore, the obtained phase can be used to correctly estimate the coupling strength (Fig. 1 orange open circles).

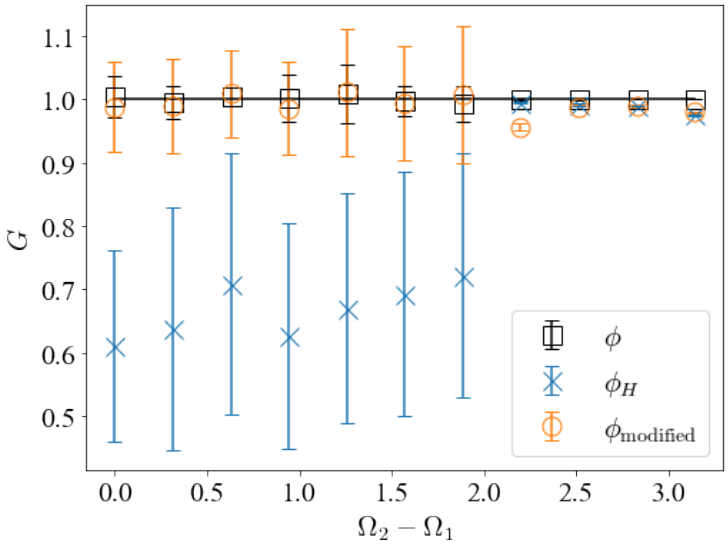

Figure 1: Estimated value of coupling strengths G are plotted against the difference of natural frequencies $\Omega_2 - \Omega_1$ between coupled two oscillators. When the phases obtained by the Hilbert transform are used in the estimation (blue cross marks), the errors and standard deviations are large, especially when $\Omega_2 - \Omega_1 < 2.0$, i.e. two oscillators are coupled. On the other hand, when using the phases estimated by our method (orange open circles), the estimation accuracy is improved.

References

[1] Michael G Rosenblum and Arkady S Pikovsky. Detecting direction of coupling in interacting oscillators. *Physical Review E*, 64(4):045202, 2001.

[2] Michael G Rosenblum, Laura Cimponeriu, Anastasios Bezerianos, Andreas Patzak, and Ralf Mrowka. Identification of coupling direction: application to cardiorespiratory interaction. *Physical Review E*, 65(4):041909, 2002.

[3] Björn Kralemann, Laura Cimponeriu, Michael Rosenblum, Arkady Pikovsky, and Ralf Mrowka. Phase dynamics of coupled oscillators reconstructed from data. *Physical Review E*, 77(6):066205, 2008.

[4] Yoshiki Kuramoto. *Chemical oscillations, waves, and turbulence*. Courier Corporation, 2003.

[5] Arkady Pikovsky, Jurgen Kurths, Michael Rosenblum, and Jürgen Kurths. *Synchronization: a universal concept in nonlinear sciences*. Cambridge university press, 2003.

[6] Björn Kralemann, Arkady Pikovsky, and Michael Rosenblum. Detecting triplet locking by triplet synchronization indices. *Physical Review E*, 87(5):052904, 2013.

Instantaneous Firing Rate Dispersion Can Decrease With Increasing Inter-spike Interval Variability

Rimjhim Tomar[1,2] and Lubomir Kostal[1]
(1) – Department of Computational Neuroscience,
Institute of Physiology, Czech Academy of Science, Prague, Czech Republic
(2) – Second Medical Faculty, Charles University, Prague, Czech Republic

One of the open questions in computational neuroscience is whether the apparent stochastic nature of neuronal activity contributes to the information processing or is a part of the intrinsic noise [1, 2]. The notions of variability and randomness of inter-spike intervals (ISI) have been proposed and studied [3] for this purpose. The analysis of ISIs only covers the temporal characteristics of the spiking data and additional methods are needed to extend this analysis to the rate coding perspective [4]. In this article we focus on the classical concept of the instantaneous firing rate [5], which is based on both the spike timing and rate coding perspectives [6] (Figure A).
We consider different spiking regimes corresponding to several standard statistical ISI models of neuronal activity and we study the probability distributions of the instantaneous firing rate [7] (Figure B). Furthermore we use different indices of statistical dispersion [3] to determine the variability and randomness of the instantaneous firing rate in each case.
We find that the relationship between the variability of the ISIs and the instantaneous firing rate is not monotonous in general. Counter-intuitively, an increase in the randomness (based on entropy) of spike times may either decrease or increase the randomness of instantaneous firing rate, in dependence on the neuronal firing model (Figure B) [7]. We apply our theoretical methods to experimental data and report that the instantaneous rate analysis may provide additional information about the spiking activity based on the ISIs. Our findings point towards the ambiguous nature of rate- and temporal-based qualities of the neuronal signal.

References

[1] R. B. Stein, E. R. Gossen, and K. E. Jones, "Neuronal variability: noise or part of the signal?," *Nature Reviews Neuroscience*, vol. 6, pp. 389–397, 2005.

[2] D. H. Perkel and T. H. Bullock, "Neural coding," *Neurosciences Research Program Bulletin*, 1968.

[3] L. Kostal, P. Lansky, and O. Pokora, "Measures of statistical dispersion based on shannon and fisher information concepts," *Info. Sci.*, vol. 235, pp. 214–223, 2013.

[4] K. Rajdl, P. Lansky, and L. Kostal, "Entropy factor for randomness quantification in neuronal data," *Neural Networks*, vol. 95, pp. 57–65, 2017.

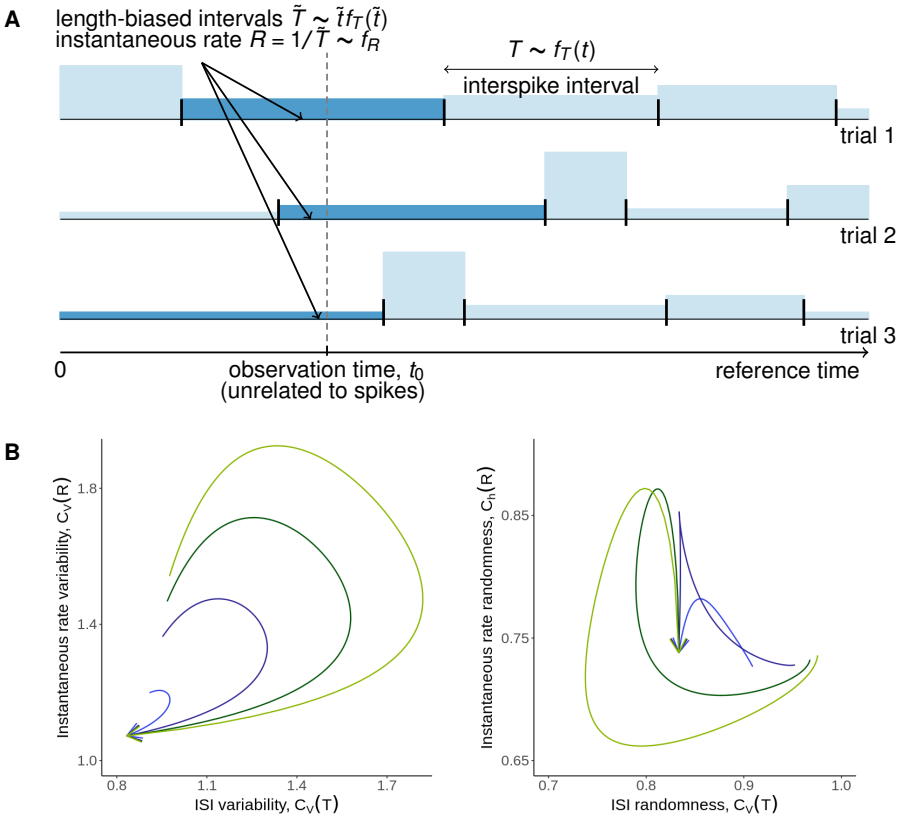

Figure: **(A)** An overview of the independent and identically distributed ISIs $T \sim f_T(t)$, under steady state conditions. The length-biased intervals $\tilde{T} \sim \tilde{t} f_T(\tilde{t})$ are observed at a fixed reference time t_0 and the inverse of $\tilde{T}$ is used to define the instantaneous rate $R \sim f_R$ with the property that $\mathbb{E}(R) = 1/\mathbb{E}(T)$. (**B**) Comparison of the dispersion measure of the ISIs and instantaneous rate for the mixture distribution with of two exponentials with a fixed refractory period, varying weight of probability components in the direction of the arrows, and varying values of the rate paratmeter of the second component b, while the first one is fixed.

[5] P. Bessou, Y. Laporte, and B. Pages, "A method of analysing the responses of spindle primary endings to fusimotor stimulation," *J. Physiol.*, vol. 196, p. 37, 1968.

[6] L. Kostal, P. Lansky, and M. Stiber, "Statistics of inverse interspike intervals: The instantaneous firing rate revisited," *Chaos*, vol. 28, p. 106305, 2018.

[7] R. Tomar and L. Kostal, "Variability and randomness of instantaneous firing rate," *Front. Comput. Neurosc.*, Accepted.

Image processing in a cerebellum like structure

Angel A. Caputi[1], Alejo Rodríguez-Cattáneo[2], Ana Carolina Pereira[3] ,Pedro A. Aguilera[4]

(1) (caputiangel@gmail.com) Unidad de Neurociencias Integrativas y Computacionales (UNIC). Instituto de Investigaciones Biológicas Clemente Estable, Av. Italia 3318, Montevideo, Uruguay

(2) (rcalejo@gmail.com) UNIC-IIBCE, Av. Italia 3318; Montevideo, Uruguay

present addresss: Facultad de Medicina, General Flores 2515, Montevideo, Uruguay

(3) (carolinapereiralarronde@gmail.com) UNIC-IIBCE, Av. Italia 3318; Montevideo, Uruguay

present addresss: Consejo de Formación en Educación, Montevideo, Uruguay

(4) (peaabar@gmail.com) Unidad de Neurociencias Integrativas y Computacionales (UNIC). Instituto de Investigaciones Biológicas Clemente Estable, Av. Italia 3318, Montevideo, Uruguay

Introduction: Electric fish explore their near environment polarizing their surroundings with an electric organ discharge (EOD). Impedance inhomogeneities perturb the field projecting an electric image to the fish skin, characteristically covered by electroreceptors. The electrosensory lobe (ELL) is the first neural relay for processing such electric images. In *Gymnotus omarorum* this structure incorporates two electrosensory paths originated in two different electroreceptor types. A fast path in which primary afferents contact a set of spherical neurons (black contacted by a green calix, Fig. 1) which directly project onto the mesencephalon, and a slow pathway, a cerebellum-like circuit of columnar organization that compares a somato-topically organized input with central expectations. The anatomy of one of these columns is schematized in Fig. 1. The main comparators are pyramidal neurons differentiated anatomically by the presence (basilar BP) or absence (non-basilar NBP) of a basilar dendritic process contacted directly by afferents. Besides these differences BP and NBP show different intrinsic properties [1].

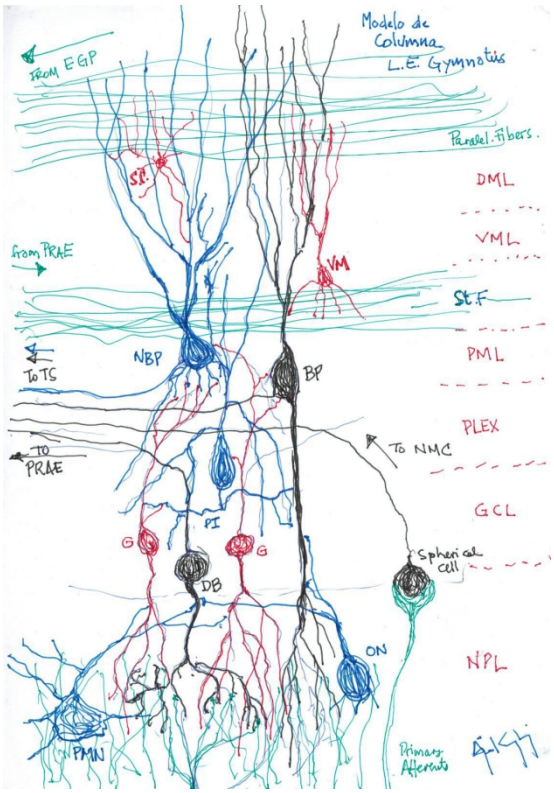

Methods: Using unitary recordings in self-discharging descerebrated preparations [2], here we address the following questions: a) Is there a frame to frame (i.e. EOD to EOD) encoding of electric images? b) What is the role of spike timing in signal encoding? c) Given that these fish show strong novelty responses to changes in the impedance of an object, does this detection occurs at the electrosensory lobe?. Modelling was performed according the connectivity shown in Fig. 1 using a mixed strategy. While the deep neurons were simulated as leaky-integrating-and-fire units, the intrinsic properties of the pyramidal neurons were simulated by a Hodgkin and Huxley-like model that accounted for the pacemaker and spike firing adaptation properties of the NBP and the slow rising excitability of BP. The input was modelled as a train of high frequency spikes modulated in spike number and intratrain frequency by stimulus intensity and showing spike firing adaptation as it was shown previously [3]

Results: Two main types of units were found in the ELL: a) one-to-one units are located at the deep neuropile (NP) firing at about 5 ms after the EOD and hardly modulated by local stimuli; b) phase preference units fire once every 2 or 3 EODs at rest but can increase their response up to three per inter-EOD-interval in the absence of nearby objects. These units can be classified by their post EOD histograms. Varying from the unit type to type, in general 3 preferential firing intervals after the EOD; one at about 5–7 ms, a second one surrounding 12–13 ms and a third one after 20 ms. All neurons showed a silence between 7 and 9 ms suggesting the presence of a strong post-EOD inhibition. The relative magnitude of the peaks at each of the three modes can be used as a main defining feature of the functional neuron type (Fig. 2).

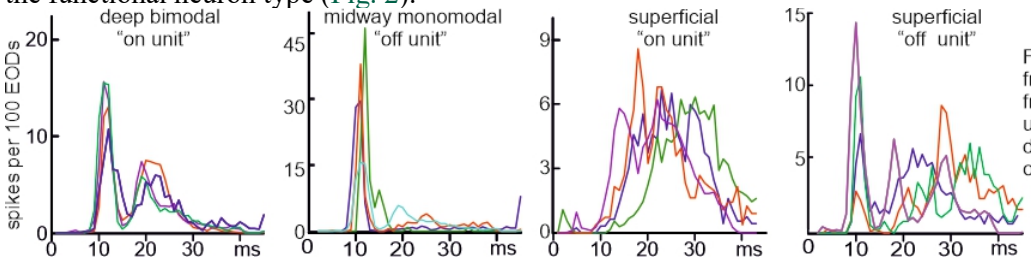

Fig. 2 Superimposed frequency polygons from four types of units recorded at different cell layers of the ELL

Post-EOD histograms of those units recorded from the centro-medial map using a multiprobe electrode placed perpendicular to the layers allowed to associate firing patterns and neuron somata locations in the electrosensory lobe layers and classify these neurons in functional types (Fig. 2).

The characteristic peaks of a neuron type are modulated differently when objects of similar shape but different impedance are placed at the same site (Fig 3 A and B). The earliest firing period showed tonic changes with object movements, while the intermediate and late periods were often dependent on the present input and previous history of stimulation. Consistently, when provoking novelty responses by the increment of the impedance of an object stationary with respect to the fish body, the probability and latency increased or decreased as a function of the change in impedance in a stepwise manner and show a gradual return to a baseline (phasic-tonic adaptation, Fig. 3C).

Simulations showed that different parameter combinations can satisfy the stationary patterns and suggests a frame-to-frame image encoding in the spike firing patterns. However, our data suggest that additional components (for example fast feedback from PRAE or synaptic plasticity at parallel fibers apical dendrites of pyramidal neurons) should be further explored and included in the model to account for the dynamics of the post EOD pattern adaptation.

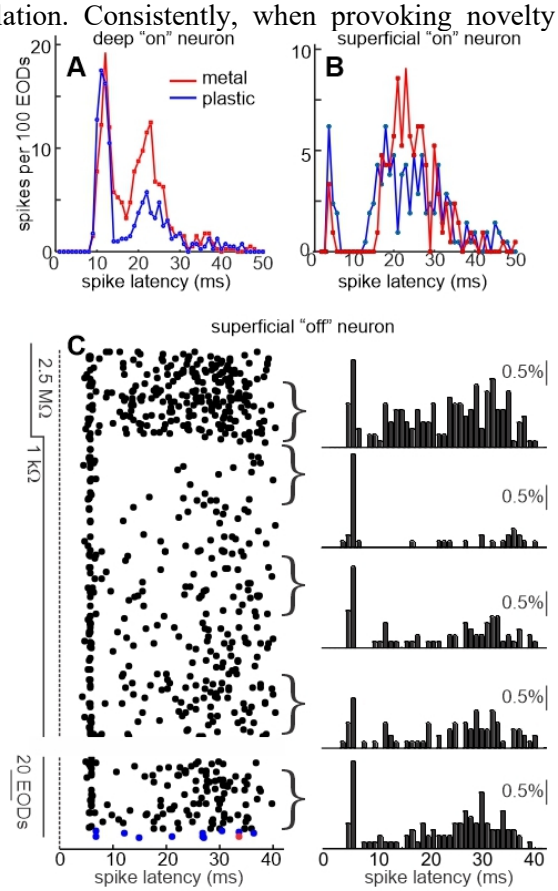

Fig 3. Spike pattern modulation. Comparison of frequency polygons when a probe cylindric object in front of the receptive field object had a plastic or a metal core. A) Deep "on" unit, B) Superficial "on" unit. C) Dynamics of spike pattern when the core of a cylindric probe is varied in a step-like fashion from 2.5 MΩ to 1kΩ.

References

[1] Nogueira, J., Castelló, M.E., Lescano, C. and Caputi, Á.A., Distinct neuron phenotypes may serve object feature sensing in the electrosensory lobe of *Gymnotus omarorum*. *J..Exp.Biol*, *224*(9), p.jeb242242. 2021.

[2] Pereira, A.C., Rodríguez-Cattáneo, A., Caputi, A.A., The slow pathway in the electrosensory lobe of *Gymnotus omarorum*: field potentials and unitary activity. J. Physiol. Paris. 108, 71–83. 2014.

[3] Rodríguez-Cattáneo, A., Aguilera, P.A., Caputi, A.A. Waveform sensitivity of electroreceptors in the pulse-type weakly electric fish *Gymnotus omarorum*. J. Exp. Biol. 220 1663–1673. 2017.

Estimating synaptic connectivity from parallel spike trains *

Ryota Kobayashi[1,2,3] and Daisuke Endo[4], and Shigeru Shinomoto[5,4]

(1) Graduate School of Frontier Sciences, The University of Tokyo

(2) Mathematics and Informatics center, The University of Tokyo

(3) JST, PRESTO

(4) Graduate School of Informatics, Kyoto university

(5) ATR Institute International

State-of-the-art techniques allow researchers to record large numbers of spike trains in parallel for many hours. In particular, the number of simultaneously recorded neurons has been doubled every seven years [1]. Such recordings allow us to infer the fine structure of neural circuits, that is, the synaptic connectivity between neurons.

The Cross-Correlation (CC) method is a standard method for estimating the connectivity from parallel spike trains [2]. While the CC method has been used to estimate neuronal connectivity, its estimate becomes unreliable when the neural activity fluctuates largely. Previous works have extended the CC method to overcome this issue [3, 4]. For instance, Amarasingham et al. proposed to jitter the timestamps of spikes and to compare the jittered cross-correlogram to the original one [4]. However, it is still challenging to estimate the synaptic connectivity from parallel spike trains *in vivo* that usually exhibit large fluctuations.

In this contribution, we propose two approaches to resolve this large fluctuation problem: Generalized Linear model for Cross-Correlation (GLMCC) [5] and COnvolutional Neural Network for Estimating synaptic ConnecTivity (CONNECT) [6]. Both methods are extensions of the CC method. While GLMCC estimates the synaptic connectivity by fitting a Point process model to the cross-correlation data, CONNECT estimates it by using a neural network that outputs the connectivity from the cross-correlogram. We demonstrate that these methods can robustly estimate the synaptic connectivity from parallel spike trains by applying it to two synthetic datasets generated by the Hodgkin-Huxley model and the multi-timescale adaptive threshold model [7, 8]. We also evaluate the estimation performance of the proposed methods and existing methods, including the jittering method [4]. The proposed methods (GLMCC and CONNECT) performed better than the conventional methods. A ready-to-use version of the web application, the source code, and example data sets are available on our website [9].

*We thank Masahiro Naito for his technical assistance in developing a web-application program. R.K. is supported by JSPS KAKENHI Grant Numbers JP17H03279, JP18K11560, JP19H01133 and JPJSBP120202201, and JST PRESTO Grant Number JPMJPR1925, Japan. S.S. is supported by JST CREST Grant Number JPMJCR1304, and the New Energy and Industrial Technology Development Organization (NEDO).

References

[1] Stevenson, I. H., and K.P. Kording, K. P. How advances in neural recording affect data analysis. *Nature Neuroscience*, 14: 139-142, 2011.

[2] D. H. Perkel, G. L. Gerstein, and G. P. Moore, Neuronal spike trains and stochastic point processes. II. Simultaneous spike trains. *Biophysical Journal*, 7: 419-440, 1967.

[3] K. Toyama, M. Kimura, and K. Tanaka, Cross-correlation analysis of interneuronal connectivity in cat visual cortex. *Journal of Neurophysiology*, 46, 191-201, 1981.

[4] A. Amarasingham, M. T. Harrison, N. G. Hatsopoulos, and S. Geman, Conditional modeling and the jitter method of spike resampling. *Journal of Neurophysiology*, 107, 517-531, 2012.

[5] R. Kobayashi, S. Kurita, A. Kurth, K. Kitano, K. Mizuseki, M. Diesmann, B.J. Richmond, and S. Shinomoto. Reconstructing neuronal circuitry from parallel spike trains. *Nature Communications*, 10: 4468, 2019.

[6] D. Endo, R. Kobayashi, R. Bartolo, B.B. Averbeck, Y. Sugase-Miyamoto, K. Hayashi, K. Kawano, B.J. Richmond, and S. Shinomoto. A convolutional neural network for estimating synaptic connectivity from spike trains. *Scientific Reports*, 11: 12087.

[7] R. Kobayashi, Y. Tsubo, and S. Shinomoto. Made-to-order spiking neuron model equipped with a multi-timescale adaptive threshold. *Frontiers in computational neuroscience*, 3: 9, 2009.

[8] R. Kobayashi and K. Kitano. Impact of slow K^+ currents on spike generation can be described by an adaptive threshold model. *Journal of computational neuroscience*, 40, 347-362, 2016.

[9] M. Naito, R. Kobayashi, and S. Shinomoto Reconstructing neuronal circuitry from spike trains. `https://s-shinomoto.com/CONNECT`

Inhibitory noise decreases membrane potential fluctuations and may lead to increased firing regularity*

Tomas Barta[1] and Lubomir Kostal[2]

(1) – Institute of Physiology of the Czech Academy of Sciences, Prague, Czech Republic

Charles University, First Medical Faculty, Prague, Czech Republic

Institute of Ecology and Environmental Sciences, INRA, Versailles, France

(2) – Institute of Physiology of the Czech Academy of Sciences, Prague, Czech Republic

Inhibitory input to neurons increases synaptic current fluctuations. This has led to the conclusion that inhibition contributes to the high spike-firing irregularity observed in vivo [2]. However, it has been observed experimentally that evoked inhibitory input to the neuron may decrease its membrane potential fluctuation [1], due to the shunting effect of the inhibition. In our study we seek to explain why the shunting effect can overpower the noise from increased synaptic current fluctuations and whether the inhibitory input could actually lead to more regular spike firing.

We used single compartmental neuronal models to show that evoked inhibitory input decreases the membrane potential fluctuations if the signal to noise ratio of the input scales slower than the square of the input intensity, a condition which is implicitly satisfied for the Poisson shot noise. Moreover, we show that in order to reproduce this behavior in neural models, reversal potentials and synaptic filtering has to be included in the model of the synaptic input. Both properties are commonly omitted to allow for an easier analytical treatment.

To understand whether the decreased membrane potential fluctuations can lead to higher spike-firing regularity, we used models with different spike-firing adaptation (SFA) mechanisms. When SFA was implemented through ionic currents or not at all, higher levels of inhibition led to lower firing regularity, despite the decreased membrane potential fluctuations. On the other hand, we observed that evoked inhibition leads to more regular firing (while keeping the mean firing rate unchanged), if the neuron exhibits a dynamic spike firing threshold (Fig. 1E). See [3] for the published version of the presented work.

References

[1] C. Monier, F. Chavane, P. Baudot, L. J. Graham, and Y. Frégnac. Orientation and Direction Selectivity of Synaptic Inputs in Visual Cortical Neurons. *Neuron*, 37(4):663–680, 2 2003.

[2] N. Brunel. Dynamics of Sparsely Connected Networks of Excitatory and Inhibitory Spiking Neurons. *J. Comput. Neurosci.*, 8:183–208, 2000.

[3] T. Barta and L. Kostal. Regular spiking in high-conductance states: The essential role of inhibition. *Phys Rev E*, 103(2):022408, 2 2021.

*This work was supported by Charles University, project GA UK No. 1042120 and the Czech Science Foundation, project 20-10251S.

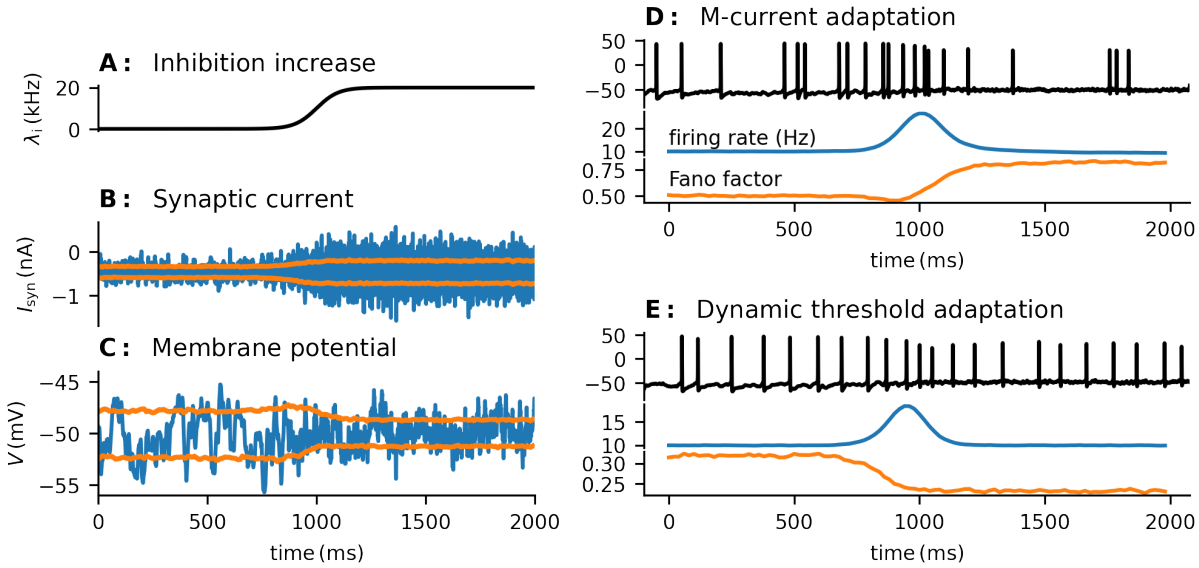

Figure 1: The increase in inhibitory input (A) increases the fluctuations of the synaptic current (B), but decreases the fluctuations of the membrane potential of a non-spiking membrane(C). The pre-synaptic spike trains are modeled as Poisson point processes. When a spike-firing mechanism is implemented, the evoked inhibition decreases the firing regularity (increases the Fano factor, orange trace) in a model with M-current SFA (D), but increases the firing regularity in a model with dynamic threshold (E). For illustration, the steady state firing rate (blue trace) is kept approximately constant by properly scaling the excitatory input.

Cointegration analysis of EEG signals*

Marie Levakova and Susanne Ditlevsen
Department of Mathematical Sciences, University of Copenhagen
Universitetsparken 5, DK 2100, Copenhagen, Denmark

Recordings obtained during EEG sessions are an invaluable source of information about activity of neuronal systems on a global level and the statistical toolbox to handle this kind of data has been growing over the last decades, with techniques focusing both on time and frequency domain. The aim of our work is to enrich the toolbox with a statistical methodology suited to investigate the functional network structure of the EEG channels setup. The cointegration methodology has been originally developed with econometrics applications in mind [1], however, the idea to use cointegration in realm of phase-coupled oscillating systems in physics [2] and in neuroscience in particular [3] has emerged recently.

We assume that the generating process of EEG signals is a system of coupled Ornstein-Uhlenbeck processes, which implies that observations in discrete time points are an integrated (nonstationary) vector autoregressive (VAR) process. The idea of cointegration analysis is to discern which part of the trending behavior in the data can be attributed to stochastic trends of random-walk type and which part stems from long-term linear equilibrium relationships, termed cointegration relationships.

The estimation procedure offers a couple of possibly interesting parameters: the *cointegration rank* gives the number of independent cointegration relationships and the number of independent stochastic trends; the *cointegration matrix* contains coefficients of cointegration relationships; and the *loading matrix* describes how the system reacts to deviations from the cointegration relationships. Most importantly, the product of the loading matrix and the cointegration matrix describes the functional network structure of the channels.

The estimation procedure, known as Johansen's procedure [4], has been designed for dimensions up to 10, which is a limit that EEG data exceed by far. The issue of high dimension is probably the biggest, but not the only technical aspect that needs to be addressed before the cointegration methodology can become a regular statistical procedure for EEG data. The results from applying cointegration analysis to a real dataset from a visual task experiment with human participants as well as challenges encountered so far will be presented.

References

[1] C. W. Granger. Some properties of time series data and their use in econometric model specification. *J. Econometrics*, 16(1): 121–130, 1981.

[2] R. Dahlhaus, I. Z. Kiss. J. C. Neddermeyer. On the Relationship between the Theory of Cointegration and the Theory of Phase Synchronization. *Statist. Sci.*, 33(3): 334–357, 2018.

*The project has received funding from the European Union's Horizon 2020 research and innovation programme under the Marie Sklodowska-Curie grant agreement No. 887784.

[3] J. Østergaard, A. Rahbek, and S. Ditlevsen. Oscillating systems with cointegrated phase processes. *J. Math. Biol.*, 75(4): 845–883, 2017.

[4] S. Johansen. *Likelihood-Based Inference in Cointegrated Vector autoregressive Models*. Oxford University Press, 1996.

Gaze-evoked nystagmus with centripetal drifts and centrifugal microsaccades during gaze fixation and its minimal neuromechanical model

Makoto Ozawa, Yasuyuki Suzuki, Taishin Nomura
Department of Mechanical Science and Bioengineering, Graduate School of Engineering Science, Osaka University

Fluctuation of gaze during gaze fixation at a desired position is composed of the drifts-tremor (DRT) and microsaccades (MS). Neural mechanisms underlying such fixational eye movement (FEM) have not been well understood. Notably, during fixation at a point laterally far from the center of the face with a large gaze angle, stochastic oscillatory motion can be observed, referred to as the gaze-evoked nystagmus (GEN). GEN typically consists of centripetal DRT and centrifugal MS, and the DRT absolute velocity and GEN occurrence rate increase according to the increase in the gaze angle [1-3]. Not a few healthy subjects exhibit GEN at small gaze angles less than 20° [1]. GEN may be the universal instability of the oculomotor system. This study aims to clarify the origin of the stochastic GEN. To this end, we quantified the GEN in terms of stochastic time series analysis, and constructed a minimal neuromechanical model of GEN. First, FEMs at five horizontal gaze angles (-15.2°, -7.76°, 0°, 7.76°, 15.2°) for 35 seconds were measured from eight healthy subjects. Each FEM time series was decomposed into DRT and MS time series. Then, we estimated the centripetal DRT horizontal velocity by estimating the slope of the regression line of the DRT time series. Similarly, the counter effect of MS was quantified by the slope of the regression line of the MS time series, which is determined by the jump width and occurrence frequency. As a result, we confirmed DRT and MS have the centripetal and centrifugal trends, respectively, and the absolute drift velocity of each trend was about 0.1 [°/s] at most, which was consistent with previous studies that assessed the tendency of centripetal DRT in other ways [2-3]. We then constructed a model using a rigid-body eyeball and Hill-type muscle models of horizontal extraocular muscles. We assumed that the globe is restricted to rotate only horizontally, and only two identical muscle models (corresponding to the lateral and medial rectus) are attached to each side of the globe, where a force balance between two antagonist muscles provides a basis of the gaze fixation and FEM. Viscoelasticity of the mechanical components was identified based on measurement studies of the mechanical parts of human eye movements [4-5]. We then argued that simulating GEN during FEM based solely on simple mechanical models with motor noise is not easy, leading to a hypothesis on intermittency in the motor commands for antagonistic muscles. Finally, we propose a minimal model for simulating GEN.

References

[1] C. A. Whyte, A. M. Petrock, and M. Rosenberg, Occurrence of physiologic gaze-evoked nystagmus at small angles of gaze, *Investigative ophthalmology & visual science*, 51(5): 2476-2478, 2010.
[2] M. Eizenman, P. Cheng, J. A. Sharpe, and R. C. Frecker, End-point nystagmus and ocular drift: an experimental and theoretical study, *Vision Research*, 30(6): 863-877, 1990.
[3] G. Bertolini, A. A. Tarnutzer, I. Olasagasti, E. Khojasteh, K. P. Weber, C. J. Bockisch, D. Straumann, and S. Marti, Gaze holding in healthy subjects, *PLoS ONE*, 8(4): e61389, 2013.
[4] D. A. Robinson, D. M. O'Meara, A. B. Scott, and C. C. Collins, Mechanical components of human eye movements, *Journal of Applied Physiology*, 26(5): 548-553, 1969.
[5] D. S. Childress and R. W. Jones, Mechanics of horizontal movement of the human eye, *The Journal of Physiology*, 188(2): 273-284, 1967.

Qualitative properties of numerical methods for the inhomogeneous geometric Brownian motion*

Irene Tubikanec[1], Massimiliano Tamborrino[2], Petr Lansky[3] and Evelyn Buckwar[4]

(1) – Institute of Stochastics, Johannes Kepler University Linz

(2) – Department of Statistics, University of Warwick

(3) – Institute of Physiology, Czech Academy of Sciences

(4) – Institute of Stochastics, Johannes Kepler University Linz

The inhomogeneous geometric Brownian motion (IGBM) is used to model changes in the membrane voltage of a neuron between two consecutive spikes [1]. It is a member of the class of Pearson diffusions, and characterised by an inhomogeneous drift term. Different from other well-known Pearson diffusions, such as the Ornstein-Uhlenbeck process and the square-root process (also known as Feller process), no method of exact simulation is known for the IGBM. In this talk, we analyse and compare qualitative features of different numerical methods for the IGBM [2]. The conditional and asymptotic mean and variance of the IGBM are known and the process can be characterised according to Feller's boundary classification. We compare the frequently used Euler-Maruyama and Milstein methods, two Lie-Trotter and two Strang splitting schemes and two methods based on the ordinary differential equation (ODE) approach, namely the classical Wong-Zakai approximation and the recently proposed log-ODE scheme. First, we prove that, in contrast to the Euler-Maruyama and Milstein schemes, the splitting and ODE schemes preserve the boundary properties of the process, independently of the choice of the time discretisation step. Second, we derive closed-form expressions for the conditional and asymptotic means and variances of all considered schemes and analyse the resulting biases. While the Euler-Maruyama and Milstein schemes are the only methods which may have an asymptotically unbiased mean, the splitting and ODE schemes perform better in terms of variance preservation. The Strang schemes outperform the Lie-Trotter splittings, and the log-ODE scheme the classical ODE method. The mean and variance biases of the log-ODE scheme are very small for many relevant parameter settings. However, in some situations the two derived Strang splittings may be a better alternative, one of them requiring considerably less computational effort than the log-ODE method.

References

[1] G. D'Onofrio, P. Lansky, and E. Pirozzi. On two diffusion neuronal models with multiplicative noise: The mean first-passage time properties. *Chaos*, 28:043103, 2018.

[2] I. Tubikanec, M. Tamborrino, P. Lansky, and E. Buckwar. Qualitative properties of numerical methods for the inhomogeneous geometric Brownian motion. 2021. Preprint available at: https://arxiv.org/abs/2003.10193.

*This work was supported by the Austrian Exchange Service (OeAD), bilateral project CZ 19/2019 and by the Austrian Science Fund (FWF), W1214-N15, project DK 14.

Using causal information theory to characterize cortical signals during a Go/No-Go task*

Helena B. de Lucas[1], Steven L. Bressler[2], Fernanda S. Matias[1] and Osvaldo A. Rosso[1]
(1) Instituto de Física, Universidade Federal de Alagoas, Alagoas, Maceió, Brazil
(2) Center for Complex Systems and Brain Sciences, Dept. of Psychology,
Florida Atlantic University, Boca Raton,USA

The characterization of dynamic systems through the theory of causal information has been shown to be extremely important in several areas of science, as it allows to gauge unique characteristics and compare them. Specifically, this methodology has already proved useful and effective in areas such as ecology, economics, literature, neurosciences, among others. It is enough that the complex system presents a time series to apply the information theory methods.

At present, the analyzed system was the dynamic of the brain of an adult monkey measured through Local Field Potential (LFP) signals. The four regions measured were: Primary Motor cortex (Region 1) and Primary Somatosensory cortex (Region 2) and two sites in the Posterior Parietal cortex (Region 3 and 4). The data were measured during the realization of a Go/No-Go task, in which the monkey keeps his hand pressed on a lever (No-Go) or removes it (Go) depending on the visual stimulus he receives. The task was repeated 710 times and each one was divided into 11 windows with 90 milliseconds of duration each. The visual stimulus occurs at the third window, for this reason, the first and the second windows were used as the baseline to calculate mean and standard deviation of the information indices.

The objective was to verify if there are dynamic differences for each region when the monkey releases or holds its lever pressed during a task. For that, two quantifiers of the causal information theory were used, they are: Normalized Shannon Entropy ($H(P)$) and Statistical Complexity ($C(P, P_e)$) that were measured for the 11 windows of the four regions. A 2-D graph, called Causal Information Plane, was also plotted, where the axes are $C(P, P_e)$ *versus* $H(P)$, in order to obtain more information about the system. For greater precision, asymmetry indices were also calculated to take into account the difference in complexity and entropy for the Go and No-Go trials, as well as their respective means and standard deviations.

In summary, we show that the methodology used is a useful tool to characterize the information process of brain signals. We can determine cortical regions in which the specific response to information is processed and at which point in the task the response is most evident. Combined with the asymmetry index and their respective means and standard deviations, it was possible to corroborate the measurements accurately, as well as to estimate if the response time happens earlier than expected in other methodologies (such as average potential). By dividing the trials into windows, we can see the dynamic evolution for each region as the task progresses. Finally, this methodology of extract a probability density function from the system, allows us to investigate several time scales to determine a characteristic time (which maximizes the complexity) of the time series taken from the dynamic system.

*CAPES research development agency and the Physics Institute of the Federal University of Alagoas.

Figure 1 shows the causal information plane for the moment of the task (W_i) where the difference between Go and No-Go trials becomes more evident for each region. It can be said that it is in these windows that the main brain processing of these regions occurs for this type of cognitive task. These windows are also compared with W_1 (in gray), where no information processing is expected to occur. The black curves are the maximum C_{max} and minimum C_{min} curves of complexity.

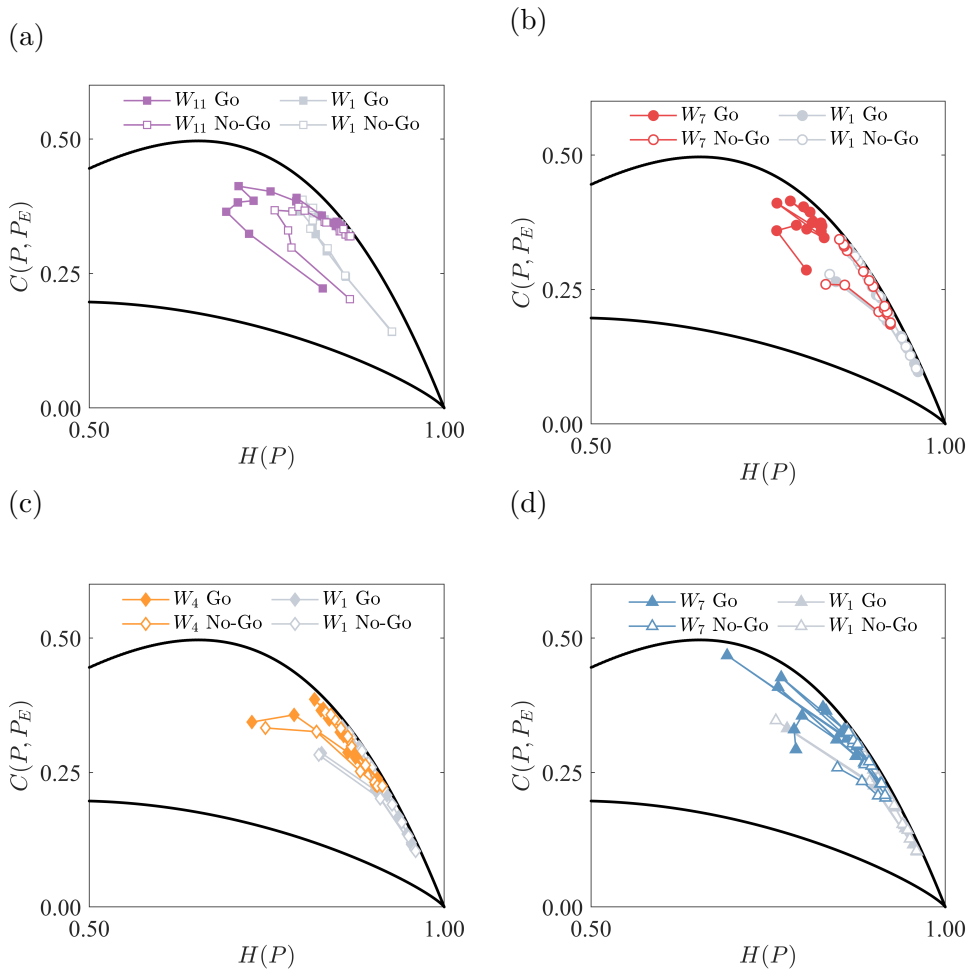

Figure 1: Multi-scale Complexity-Entropy plane for the first 15 time delays τ. For each region we depict C *versus* H values for the first window W_1 (Go and No-Go trials in grey) and a post-stimulus window that shows an illustrative separation between Go and No-Go trials in the plane. (a) Region 1: W_{11}. (b) Region 2: W_7. (c) Region 3: W_4. (d) Region 4: W_7. Solid lines in black represent the maximum and minimum complexity values for a fixed value of the entropy.

References

[1] H. B. Lucas and S. L. Bressler F. S. Matias and O. A. Rosso. A symbolic information approach to characterize response-related differences in cortical activity during a Go/No-Go task. *Nonlinear Dynamics*, 1-11, 2021. DOI: 10.1007/s11071-021-06477-1

Classifying Mild Cognitive Impairment from EEG Patterns for Dementia Onset Prediction*

Tomasz M. Rutkowski[1,2,3], Masato S. Abe[1], Seiki Tokunaga[1],
Tomasz Komendziński[3], and Mihoko Otake-Matsuura[1]
(1) – RIKEN Center for Advanced Intelligence Project (AIP), Tokyo, Japan
tomasz.rutkowski@riken.jp
(2) – The University of Tokyo, Tokyo, Japan
(3) – Nicolaus Copernicus University, Toruń, Poland

A rise in dementia cases globally significantly increases healthcare expenses. According to the World Health Organization, nearly 50 million older adults live with progressing dementia [2]. A feasible utilization of AI shall advance early prediction and following cognitive well-being improvement within the so-called "digital pharma" or "beyond a pill" non-pharmacological-therapeutical strategies.

We report pilot study results of EEG experiments with older adults in the RIKEN Center for Advanced Intelligence Project (AIP) as an extension to our previous behavioral [3] and EEG [4] studies in a passive BCI setting for dementia onset prediction through a binary classification, comparing shallow and deep machine learning (ML) models, of normal cognition versus mild cognitive impairment (MCI). The RIKEN Ethical Committee approved the study, and it adheres to The Declaration of Helsinki. The 35 elderly take part; a number of females = 22; mean age = 73.5 ± 4.85 years old. All participants receive monetary gratification, and they give written

*This research was supported in part by the KAKENHI, the Japan Society for the Promotion of Science Grant No. JP18K18140 (MSA), JP18KT0035 (MOM), JP19H01138 (MOM), JP20H05022 (MOM), JP20H05574 (MOM), and the Japan Science and Technology Agency AIP Trilateral AI Research Grant No. JPMJCR20G1 (MOM, TMR).

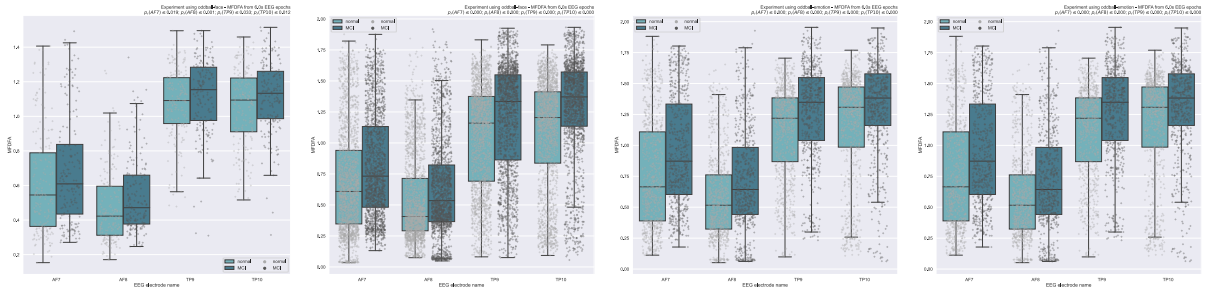

(a) Attended face $p_r \leq 0.033$ (b) Inhibited face $p_r \ll 0.000$ (c) Attended emotion $p_r \ll 0.000$ (d) Inhibited emotion $p_r \ll 0.000$

Figure 1: MFDFA feature distributions in four-channel EEG during short-video with face- and facial-emotion-short-term-memory tasks. Panels (a) and (b) present results for face oddball cases of attended and inhibited stimuli, while (c) and (d) for the same face emotional expressions. The MCI subject had significantly higher median MDFA scores as evaluated with Wilcoxon rank sums tests and shown in panel captions.

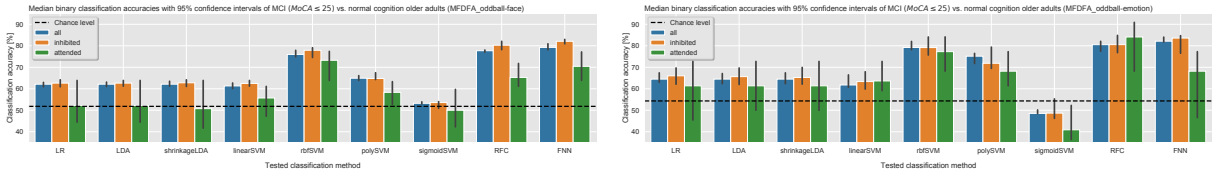

(a) Face oddball

(b) Emotional oddball

Figure 2: Classification results using shallow (linear regression – LR; linear discriminant analysis – LDA; shrinkage LDA; linear support vector machine – linear SVM; radial basis function SVM; polynomial SVM; sigmoid SVM; random forest classifier – RFC; and fully connected deep neural network (five hidden layers) – FNN). The best results are for the FNN classifier using only the inhibited MFDFA patterns for both facial and emotion stimuli oddball tasks.

informed consent. First, we apply a four-channel portable MUSE 2016 headband by InteraXon Inc., Canada. It has been shown already that the MUSE device allows for a reliable EEG capture from preset $AF7, AF8, TP9$, and $TP10$ dry electrode locations. Each participant sits in a chair in front of a computer display during the EEG experiments presenting short video stimuli ($5 \sim 7$ seconds) with facial emotional expressions. We compare two short-term memory oddball tasks with instructions given to the subjects to remember a face (different persons randomly presented in each run) and facial expressions (the same person presenting varying facial expressions in each run). Next, we calculate multifractal detrended fluctuation analysis features (MFDFA) [1] from 6 seconds post-stimulus intervals for both attended (oddball targets) and inhibited (oddball distractors) stimuli. MFDFA feature distributions for all the analyzed EEG channels we summarized in Figure 1. Finally, we classify the MFDFA patterns obtained from four EEG channels using shallow and deep learning classifiers, as explained in the caption of Figure 2. We received the best accuracy results for the FNN classifier trained in a ten-fold-cross-validation setting using only the inhibited stimuli in the face- and emotional-expression-oddball experiments with median results above 80%, which suggested that the distractor inhibition EEG patterns did vary for normal and MCI subjects.

The thriving utilization of AI/ML-based dementia onset prediction shall benefit aging societies globally. However, we also acknowledge the inherent limitations of the presented strategy as we only infer human-error-prone subjective cognitive evaluation measures rendered to binary MCI thresholds at a level MoCA $\leqslant 25$, which are only proxy indicators of dementia. Therefore, we plan to continue this line of research by combining EEG and fNIRS-based measures for a broader coverage for Alzheimer's and vascular dementia biomarker development.

References

[1] J. W. Kantelhardt, S. A. Zschiegner, E. Koscielny-Bunde, S. Havlin, A. Bunde, and H. E. Stanley. Multifractal detrended fluctuation analysis of nonstationary time series. *Physica A: Statistical Mechanics and its Applications*, 316(1-4):87–114, 2002.

[2] G. Livingston, J. Huntley, A. Sommerlad, D. Ames, C. Ballard, S. Banerjee, C. Brayne, A. Burns, J. Cohen-Mansfield, C. Cooper, S. G. Costafreda, A. Dias, N. Fox, L. N. Gitlin, R. Howard, H. C. Kales, M. Kivimäki, E. B. Larson, A. Ogunniyi, V. Orgeta, K. Ritchie, K. Rockwood, E. L. Sampson, Q. Samus, L. S. Schneider, G. Selbæk, L. Teri, and N. Mukadam. Dementia prevention, intervention, and care: 2020 report of the Lancet Commission. *Lancet*, 0(0), jul 2020.

[3] T. M. Rutkowski, M. S. Abe, M. Koculak, and M. Otake-Matsuura. Classifying mild cognitive impairment from behavioral responses in emotional arousal and valence evaluation task - ai approach for early dementia biomarker in aging societies -. In *The 42nd Annual International Conference of the IEEE Engineering in Medicine and Biology Society (EMBC)*, pages 5537–5543, Montreal, Canada, July 20–24, 2020. IEEE Engineering in Medicine and Biology Society, IEEE Press.

[4] T. M. Rutkowski, M. Koculak, M. S. Abe, and M. Otake-Matsuura. Brain correlates of task–load and dementia elucidation with tensor machine learning using oddball BCI paradigm. In *ICASSP 2019 - 2019 IEEE International Conference on Acoustics, Speech and Signal Processing (ICASSP)*, pages 8578–8582, May 2019.

Origins and consequences of serial dependence in vestibular neural models

Charles E. Smith[1]

(1) Dept. of Statistics

North Carolina State University

The firing times of neurons produce a sequence of brief electrical pulses (action potentials) that can be regarded as a stochastic point process. In this report a well-cited model (Smith and Goldberg, 1986) for the firing times of the mammalian peripheral vestibular nerve is used to examine the effect of cumulative vs noncumulative afterhyperpolariztion on the serial dependence among the resultant spike train. A non-renewal point process is indicated at moderate to high firing rates in the case of cumulative afterhyperpolarization. The dependence is Markovian and is a function of the duration of the previous interspike interval. The modelling and biological consequences of this rate dependent serial dependence in the context of neural information processing in the vestibular system (Linder et al., 2005; Rowe and Neiman, 2012;Sadeghi et al., 2007) and more general neural models (Kostal and Lansky, 2011; Tomar and Kostal, 2021) is explored.

This integrate and fire model wih a constant threshold in reduced form is given by

$$x(t) = \frac{(g_S V_S + g_K(t) V_K + V_P)}{1 + g_S + g_K(t)},$$

Where x(t) is the membrane voltage process referred to the resting level, which is set to zero. V_S and V_K are positive (synaptic) and negative (potassium) equilibrium potentials, respectively as indicate din the circuit below. The g's are normalized membrane conductances (normalized by the leakage conductance) with the $g_K(t)$ being a decaying exponential and g_S being a shot noice process produced by passing a Poisson process through a finite impulse response filter of duration 0.5 msec. V_P being the postsynaptic current source.

Cumulative afterhyperpolarization (AHP), which can make the firing times be non-renewal, is represented as follows: a fixed proportition, p, of the g_K left over from the preceding activity was added to the g_K triggered by each spike. If the (i)th interspike interval is t_i, the activity until the (i+1)th spike has a $g_K(t)$ given by

$$g_K(t) = [\, g_{K0} + p\, g_K(t_i)]\exp(-\frac{t}{\tau_K})$$

So if p is not equal zero then the initial condition for $g_K(t)$ is larger (more hyperpolarizated) than when p=0.Said another rway, the dependence of the initial value on the length of the previous interval will make the firing time a 1-memory point process. The 3 parameters (g_{K0} , g_{K0}, p) specify the AHP for a given neuron, The fourth parameter specific to each neuron is quantal epsp size, namely the mean value of $g_S V_S$ at the resting potential. We examine the cases of p=0 vs p=1 in three neurons with the other parameters as in Smith and Goldberg, 1986. The three neurons represent a regularly firing, intermediate variability and irregularly discharging fiber. The discharge rate of the neuron is

modulated by natural and electrical stimul;ation, which were mimicked by varing the mean g_S and V_P , respectively. The case with p=1 was used in Smith and Goldberg, 1986 and provided good agreement with experimental results using natural and electrical stimulation (Goldberg et al., 1984).

A moment plot the coef. of variation (CV) vs mean interspike interval (MI) is given below for the three model neurons. The solid curves (connected points) correspond to p=1 and the points correspond to p=0. The lower left corner of indicates the largest differences between p=0 and p=1. For more regularly discharging fibers the CV is larger for a given MI when p=0. Conditional mean plots and the values of the first order serial coerrlation coef. show that is region has a significant negative serial dependence. The second and third order correlation coef. are not significantly different than zero consistent with this being a first order Markov process.

The implications for neural information coding and what biological mechanisms downstream could take advantage of a reduced variablilty due to cumulative AHP are briefly examined.

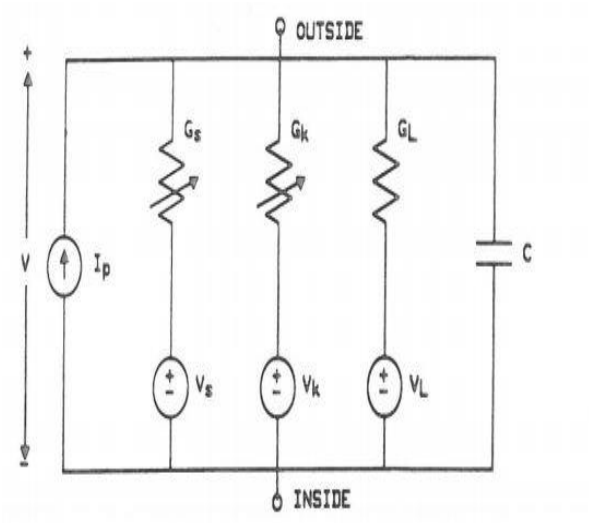

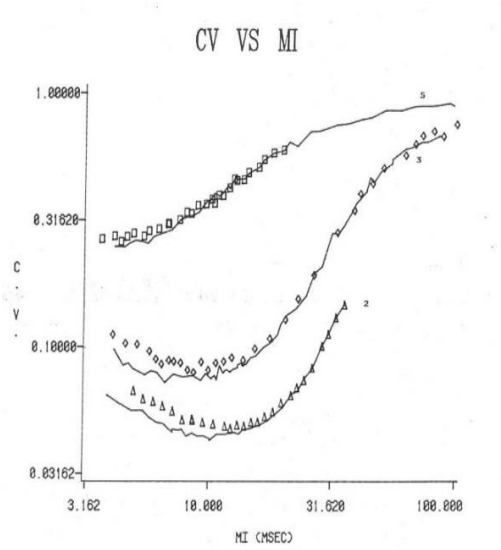

References

[1] J. M. Goldberg, C.E. Smith, and C. Fernandez, Relation between discharge regularity and responses to externally applied galvanic currents in vestibular nerve afferents of the squirrel monky, J. Neurophysiology 51: 1236-1256 (1984)

[2] L. Kostal, P. Lansky, and O. Pokora, Measures of statistical dispersion based on Shannon and Fisher information, *Info. Sci. 235: 214-223,* (2013)

[3] B. Linder, M. J. Chacron, and A. Longtin. Integrate-and-fire neurons with threshold noise: A tractable model of how interspike interval correlations affect neuronal signal transmission. *Physical Review E., 73, 021911* (2005)

[4] M. H.Rowe and A. B.Neiman, Information analysis of posterior canal afferents in the turtle, *Trachemys scripta elegans*, *Brain Research 1434:226-242*, (2012)

[5] S. G. Sadeghi, M.J. Chacron, M.C. Taylor, and K. E. Cullen,Neural Variabilty, detection thresholds, and information transmission in the vestibular system. *J. Neuroscience 27(4): 771-781*, (2007)

[6] C. E. Smith and J. M.Goldberg. A stochastic afterhyperpolarization model of repetitive activity in vestibular afferents. *Biol. Cybernetics 54:41-51* (1986).

[7] R. Tomar and L. Kostal, Variability and randomness of the instantaneous firing rate, *Frontiers in Neuroscience* (in press) 2021

Significant Spatio-Temporal Spike Patterns in Macaque Monkey Motor Cortex*

Alessandra Stella[1], Peter Bouss[1], Guenther Palm[2], Alexa Riehle[1,3], Thomas Brochier[3] and Sonja Gruen[1,4]

(1) – Institute of Neuroscience and Medicine (INM-6, INM-10), Institute for Advanced Simulation (IAS-6), and JARA Brain Institute I (INM-10), Jülich Research Centre, Jülich, Germany

(2) – Neuroinformatics, University of Ulm

(3) – Institut de Neurosciences de la Timone, UMR 7289, CNRS-AMU, Marseille, France

(4)– Theoretical Systems Neurobiology, RWTH Aachen University, Aachen, Germany

The cell assembly hypothesis [1] postulates that neurons coordinate their activity through the formation and repetitive co-activation of groups. While the classical theory of neural coding revolves around the concept that information is encoded in neuronal firing rates, we assume that assembly activity is expressed by the occurrence of spatio-temporal patterns (STPs) of spikes emitted by neurons that are members of the assembly, e.g. activating a synfire chain.

We focus on a method that is capable of detecting significant STPs in parallel spike trains, called SPADE [2, 3, 4]. SPADE first identifies repeating STPs using Frequent Itemset Mining [5], and then evaluates the detected patterns for significance through comparison to patterns found in surrogate data. Various surrogate techniques can be used to evaluate significance, and their correct choice is crucial to ensure that by-chance patterns are not classified as significant [6].

Here we first evaluate how different six types of surrogate techniques affect the results of SPADE, in terms of the general statistics of the generated surrogates, and in terms of the amount of false positives. We conclude that spike-train shifting [7] is the preferable choice for our type of data, which typically show a $CV < 1$ and have a dead time after the spikes of 1.6/1.2ms induced by the spike sorter (Plexon). Uniform dithering [8], in contrast, leads to a high false positive rate.

In a next step, we evaluate if cell assemblies are active in relation to motor behavior [2]. Therefore, we analyze 20 experimental sessions, each of about 15min recording, consisting of parallel spike data recorded by a 10x10 electrode Utah array in the pre-/motor cortex of two macaque monkeys performing a reach-to-grasp task [9, 10]. The monkeys have four possible behavioral conditions of grasping and pulling an object consisting of combinations of two possible grip types (precision or side grip) and two different amounts of force required to pull the object (low or high). We segment each session into 6 behavioral epochs of 500ms duration and analyze them independently for the occurrence of STPs. Each significant STP is identified by its neuron composition, its number and times of occurrences and the delays between spikes.

We find that significant STPs indeed occur in all phases of the behavior. Their size ranges between 2 and 6 neurons, and their maximal spatial extent is 60ms. The STPs are specific to the behavioral context, i.e. within the different trial epochs and across conditions (different grip

*Acknowledgments: The project is funded by the Helmholtz Association Initiative and Networking Fund (ZT-I-0003), by Human Brain Project HBP Grant No. 785907 (SGA2 and SGA3), and by RTG2416 MultiSenses-MultiScales (DFG).

and force type combinations). This suggests that different assemblies are active in the context of different behavior. Within a recording session, we typically find one neuron that is involved in all STPs. The neurons involved in STPs within a session are not clustered on the Utah array, but may be far apart. We further plan to investigate the spatial arrangement of the patterns on the Utah array, to determine whether there are preferred spatial directions of pattern spike sequences, as found in [2] for synchronous patterns. Finally, we plan to investigate whether the grip type can be better decoded on the basis of the type of STPs or by using the firing rates of the neurons.

References

[1] D.O. Hebb. *The organization of behavior: A neuropsychological theory* A Wiley Book in Clinical Psychology. (1949);62:78.

[2] E. Torre, P. Quaglio, M. Denker, T. Brochier, A. Riehle and S. Gruen. Synchronous spike patterns in macaque motor cortex during an instructed-delay reach-to-grasp task. *Journal of Neuroscience*, 36.32 (2016): 8329-8340.

[3] P. Quaglio, A. Yegenoglu, E. Torre, D.M. Endres, and S. Gruen. Detection and evaluation of spatio-temporal spike patterns in massively parallel spike train data with spade. *Frontiers in computational neuroscience*, 11 (2017):41.

[4] A. Stella, P. Quaglio, E. Torre, and S. Gruen. 3d-SPADE: Significance evaluation of spatio-temporal patterns of various temporal extents. *Biosystems*, 185 (2019):104022.

[5] F. Porrmann, S. Pilz, A. Stella, A. Kleinjohann, M. Denker, J. Hagemeyer and U. Rueckert. Acceleration of the SPADE method using a custom-tailored FP-growth implementation. *Submitted.*

[6] A. Stella, P. Bouss, G. Palm and S. Gruen. *In preparation.*

[7] G. Pipa, S. Gruen and C. Van Vreeswijk. Impact of spike train autostructure on probability distribution of joint spike events. *Neural Computation* 25.5. (2013):1123-1163.

[8] A. Date, E. Bienenstock and S. Geman. On the temporal resolution of neural activity. *Society for Neuroscience abstracts* Brown University, Division of Applied Mathematics (1998).

[9] T. Brochier, L. Zehl, Y. Hao, M. Duret, J. Sprenger, M. Denker, S. Gruen and A. Riehle. Massively parallel recordings in macaque motor cortex during an instructed delayed reach-to-grasp task. *Scientific Data*, 5.1 (2018): 1-23.

[10] A. Riehle, S. Wirtssohn, S. Gruen and T. Brochier. Mapping the spatio-temporal structure of motor cortical LFP and spiking activities during reach-to-grasp movements. *Frontiers in neural circuits*, 7 (2013): 48.

Strong energy component is more important than spectral selectivity in modeling responses of midbrain auditory neurons to wide-band environmental sounds*

Tsai-Rong Chang[1], Dominik Sorek[2], Petr Marsalek[3] and Tzai-Wen Chiu*[4]

(1) –1 Department of Computer Science and Information Engineering, Southern Taiwan University of Science and Technology, Taiwan, ROC;

(2) – [2] Department of Pathological Physiology, First Medical Faculty, Charles University in Prague, Czech Republic;

(3) –[2] Department of Pathological Physiology, First Medical Faculty, Charles University in Prague, Czech Republic;

(4) –[3] Department of Biological Science and Technology, National Yang Ming Chiao Tung University, Hsinchu, Taiwan, ROC

Acknowledgments: We thank Drs. Xinde Sun and Paul Poon for their technical support, helpful discussion, and reading the manuscript. This study was supported by grants from the Ministry of Science and Technology, Taiwan (Taiwan-Czech bilateral project: MOST-GARC-105-2923-B-009-001-MY3, MOST-106-2221-E-009 -173 -MY3, MOST-109-2221-E-218-022), Center For Intelligent Drug Systems and Smart Bio-devices (IDS2B) from The Featured Areas Research Center Program within the framework of the Higher Education Sprout Project by the Ministry of Education, Taiwan, Allied Advanced Intelligent Biomedical Research Center under the Higher Education Sprout Project, Ministry of Education, Taiwan, and Czech Science Foundation (16-09086J).

Modeling central auditory neurons in response to complex sounds not only helps understanding neural processing of speech signals but can also provide insights for biomimetics in neuro-engineering. While modeling responses of midbrain auditory neurons to frequency-modulated tones is rather good, modeling those to environmental sounds remains less satisfactory. Environmental sounds are typically characterized by the presence of strong energy components over a wide frequency range. The importance of such stimulus feature has not been examined in the conventional approach of auditory modeling that focuses on spectral selectivity. To this end, we manipulated the energy of two representative environmental sounds, both in power and in spectrum, to see how the responses of 25 rat auditory midbrain neurons would be affected in modeling. The environmental sound stimuli were those commonly present in a laboratory cage where a rat was either (a) drinking from a feeding bottle ('drinking sound') or (b) chewing food pellets (‘eating sound’). The spectrum of each sound was first divided into multiple non-overlapping frequency bands before presented to an artificial neural model built on a committee machine with stratified parallel inputs to simulate the known tonotopic architecture of the auditory midbrain. The model was trained to predict empirical response probability profiles of neurons to the repeated environmental sounds. Results showed that the model performance depended more on the strong energy components than on the spectral selectivity as might be conventionally expected. Findings were discussed in relation to the broadband nature of environmental sounds, and the general sensitivity of midbrain auditory neurons to rapidly changing sound intensities.

Eigenangles: evaluating the statistical similarity of neural network simulations via eigenvector angles *

Robin Gutzen[1,2], Sonja Grün[1,2], Michael Denker[1]

(1) Institute of Neuroscience and Medicine (INM-6) and Institute for Advanced Simulation (IAS-6) and JARA-Institut Brain Structure-Function Relationships (INM-10), Jülich Research Centre, Jülich, Germany

(2) Theoretical Systems Neurobiology, RWTH Aachen University, Aachen, Germany

In modern neuroscience, modeling and simulation of neuronal networks represent a powerful means to combine insights from experiments and theory into a coherent understanding of brain function. The only gauge to assess how much trust we can place in a given model is how well it can predict the biological reality it aims to describe. Validation testing formalizes the comparison between empirical data and the measures extracted from a model, e.g., using numeric simulations, and quantifies their similarity [1, 2]. In a similar fashion, these validation tests can also be used to directly compare two models, which can be beneficial in evaluating a model's robustness with respect to parameter variation, and in iteratively improving the model. Practically, these comparisons require the extraction of characteristic measures from both the model and experimental data, and statistical testing under the null hypothesis of equivalence. In particular, validation tests that evaluate the similarity of spiking network activity can be based either on single neuron measures (e.g., firing rate), pairwise measures (e.g., correlation), or higher-order measures (e.g., graph centrality). Single neuron measures can be evaluated for similarity via standard two-sample testing of the corresponding distributions. However, due to their combinatorial complexity, pairwise measures are much less straightforward to compare in a statistically rigorous manner.

Here, I present a statistical test that evaluates the similarity of pairwise measures by testing the angles between eigenvectors under the null hypothesis that the two networks don't share any distinct features that are reflected in theses measures. For correlation measures, such features can, for example, be represented by correlated sub-groups of neurons. Pairwise measures, like the Pearson correlation coefficient, are typically arranged in an NxN matrix, where N is given by the number of neurons. In the case of independent activity, this matrix can be described in terms of random matrices. One characteristic of random matrices is that their eigenvectors are randomly distributed, i.e. uniformly over the surface of an N-sphere [3]. The distribution of the angles between such random vectors can be described by a power law of a sinusoid $(\sin(\phi)^{N-2})$ [4].

The underlying idea of the proposed statistical test is that if there exists a sufficiently strong deviation from the random matrix null hypothesis, as for example, in the form of a correlation in a subset of neurons, this would cause an eigenvector to point into the direction of those neurons.

*Acknowledgements: This project has received funding from the European Union's Horizon 2020 Framework Programme for Research and Innovation under Specific Grant Agreement No. 785907 (Human Brain Project SGA2) and 945539 (Human Brain Project SGA3), DFG RTG2416 'Multi-Senses Multi-Scales', Helmholtz Association Initiative Networking and Fund under project number ZT-I-0003, and the Helmholtz School for Data Science in Life, Earth and Energy (HDS-LEE).

If such a correlated subset exists in both of the datasets entering the comparison, both would have an eigenvector pointing into a similar direction, and thus the angle between them would be small compared to the null distribution of random "eigenangles". According to this idea, the proposed statistical test measures the angles between all eigenvector pairs and weights them with the corresponding eigenvalues. Evaluating these angles under consideration of the null hypothesis yields a cumulative probability measure of whether the two datasets share similar non-random activity features.

Whereas the symmetric correlation matrices are suitable to characterize population activity, the statistical evaluation of eigenangles can be further generalized and extended to asymmetric measures, in particular connectivity matrices. While the eigenvector distribution of the connectivity matrix depends on the details of the network architecture, for several cases of simple networks the eigenvector and eigenvalue distributions can still be formally described. Moreover, while the eigenvalue distribution of symmetric matrices can be analytically described by the Marchenko-Pastur distribution [8], for the formal description of the eigenvalues of connectivity matrices Rajan and Abbott [7] found an analytical expression for the eigenvalue distribution of a certain set of networks, which can be leveraged here. Besides the application in a validation context, in combination, these measures for symmetric and asymmetric matrices furthermore provide the means to investigate quantitatively the relations between connectivity and activity.

Together with the theoretical basis of the statistical test, I demonstrate its capabilities and limitations with respect to artificial stochastic calibration data and neural network simulations. This work contributes to the effort of building software packages for validation (see, e.g., NetworkUnit, RRID:SCR_016543) to make modeling and simulation more quantitative and reproducible [5, 6].

References

[1] Schlesinger, S. "Terminology for model credibility." *Simulation 32* (1979): 103–104.

[2] Thacker, Ben H., et al. "Concepts of model verification and validation." *Los Alamos, NM: Tech. rep.* (2004).

[3] Holmes, Richard B. "On random correlation matrices." *SIAM journal on matrix analysis and applications* 12.2 (1991): 239-272.

[4] Cai, T. Tony, Jianqing Fan, and Tiefeng Jiang. "Distributions of angles in random packing on spheres." *Journal of Machine Learning Research* 14 (2013): 1837.

[5] Gutzen, Robin, et al. "Reproducible neural network simulations: statistical methods for model validation on the level of network activity data." *Frontiers in Neuroinformatics* 12 (2018): 90.

[6] Trensch, Guido, et al. "Rigorous neural network simulations: a model substantiation methodology for increasing the correctness of simulation results in the absence of experimental validation data." *Frontiers in Neuroinformatics* 12 (2018): 81.

[7] Rajan, Kanaka, and Larry F. Abbott. "Eigenvalue spectra of random matrices for neural networks." *Physical review letters* 97.18 (2006): 188104.

[8] Marchenko, Vladimir Alexandrovich, and Leonid Andreevich Pastur. "Distribution of eigenvalues for some sets of random matrices." *Matematicheskii Sbornik* 114.4 (1967): 507-536.

Characterization of inputs from filtered intracellular recordings*

George Hadjiantonis[1], Guido Bugmann[2] and Chris Christodoulou[1]
(1) Department of Computer Science, University of Cyprus, 1678 Nicosia, Cyprus
{ghadji02, cchrist}@cs.ucy.ac.cy
(2) School of Engineering, Computing and Mathematics,
University of Plymouth, Drake Circus, Plymouth PL4 8AA, United Kingdom
gbugmann@plymouth.ac.uk

Identifying the underlying presynaptic input parameters, i.e., amplitude, duration and synchronicity is required for determining the neural operational mode and for better understanding of a neuron's behavior. The general aim of this work is to propose a method of analyzing the temporal structure of the neuron's membrane potential and characterize the presynaptic input that induced it.

The proposed method measures the variability of a filtered version $V_F(t, \Delta t)$ of the membrane potential $V(t)$, using a filter that compares the potential at the time t with that at time $t + \Delta t$ and $t - \Delta t$; $V_F(t, \Delta t) = V(t) - (V(t - \Delta t) + V(t + \Delta t))/2$. This filtered version of the membrane potential is sensitive to the correlation between signals at different temporal distances and for small Δt it is essentially a peak detector. The variability of the filtered membrane potential is the standard deviation of V_F over a given data time window.

We first investigated how the variability is affected by the different features of the presynaptic input, namely amplitude, frequency, duration (time to peak) and synchrony of individual events, using simulated data. Each parameter was examined separately through simulations of uniformly or randomly distributed alpha functions. For a series of isolated peaks of the simulated potential, the variability was highest for filter time interval Δt equal to the duration of the peaks. By increasing the duration of the individual alpha functions, we noted a slower increase of variability with a filter time interval. Moreover, for randomly timed peaks of constant rate, the variability remained relatively at the same level after reaching a certain maximum value. There was also a clear correlation between the height of the peaks and the variability.

We then applied our proposed method to experimental data. The experimental data used for this work consisted of intracellular recordings from cats' V1 simple cells, previously described in [1]. Neurons were stimulated by monocularly presented drifting sine-wave gratings. According to the push-pull architecture of the input to V1 simple cells, when a grating of optimal spatial frequency and orientation is presented over the receptive field, the V1 cell receives alternately strong excitatory and inhibitory input. This property allowed us to separately examine the effects of excitation and inhibition. We divided the postsynaptic membrane potential into two different periods based on neuron's resting potential: pre-spiking period, starting from the resting potential until the first spike of each burst and inhibitory period, when the membrane potential is below

*We would like to thank Professor Matteo Carandini (University College London, University of London, UK) for kindly providing us the experimental data, without which this work would not have been possible.

the resting potential. Part of the experimental data and the two periods are illustrated in Fig. 1 (Left). The results, shown in Fig. 1 (Right) with solid lines, suggest shorter duration and higher amplitudes for Excitatory Postsynaptic Currents (EPSC) and longer duration and lower amplitudes for Inhibitory Postsynaptic Currents (IPSC).

Based on these results we set the parameters of a simulation, to attempt to reproduce the variability of real neurons. For the simulation we used a Leaky Integrate and Fire model (LIF), with injected current as the sum of alpha functions, representing the individual presynaptic inputs. The time of the alpha functions was determined by two Poisson processes, one for excitation and one for inhibition, whose rates were modulated at the same frequency (4 Hz) as the presentation of the stimulus gratings, and out of phase. The variability of the simulated data is shown in Fig. 1 (Right) with dashed lines.

We are currently further examining the effects of input synchrony and the possibility of a connection with the oscillations observed in the variability of the pre-spiking period of the real neuron.

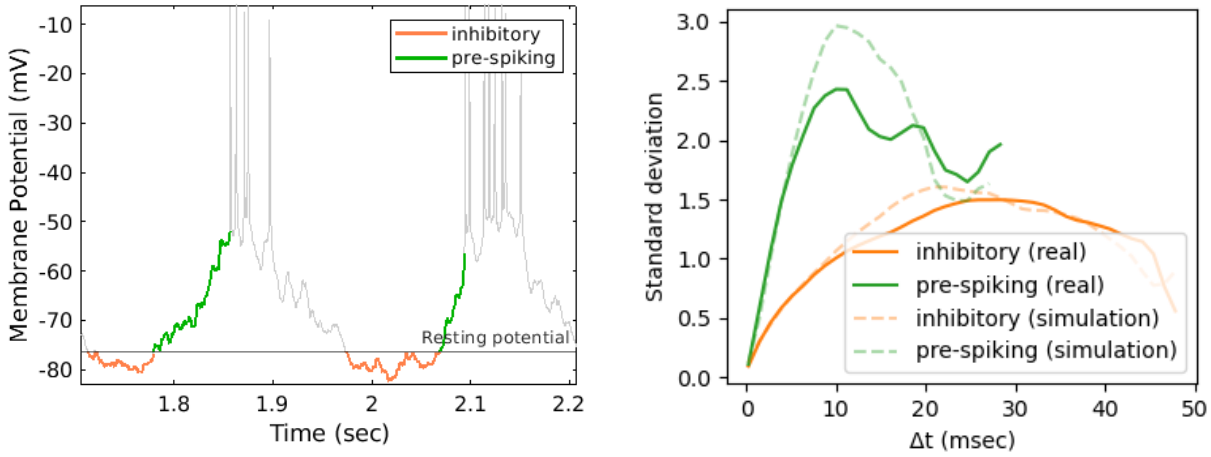

Figure 1: (Left) Membrane potential of a V1 simple cell, stimulated at the preferred orientation. (Right) Variability of the experimental (solid lines) and simulated data (dashed lines). The simulation consisted of a LIF model, with time constant of 12 msec. For simplicity we assume $R = 1m\Omega$ and the postsynaptic currents (EPSC and IPSC) generated by input spikes were simulated as a sum of alpha functions with amplitudes in units of mV. Excitatory inputs are Poisson spike trains with a maximum rate of 750 Hz that trigger individual alpha currents (EPSC) with amplitude $A = 10mV$ and time to peak of $TTP = 1.4msec$. Inhibitory inputs have a maximum rate of 100 Hz and trigger alpha functions with amplitude of $A = -5mV$ and $TTP = 2msec$.

Reference

[1] Carandini, M., and Ferster, D. Membrane potential and firing rate in cat primary visual cortex. *Journal of Neuroscience.* 2000, 20(1):470-84.

The Difference Neuron: A versatile abstract spiking neuron model

Jacob Kanev[1], Achilleas Koutsou[2], Chris Christodoulou[2] and Klaus Obermayer[1]
(1) – Faculty IV, Institute of Software Engineering and Theoretical Computer Science,
Neural Information Processing Group, Berlin University of Technology, Germany
(2) – Department of Computer Science, University of Cyprus, Cyprus

Neurons calculate their response to their stimulus at different time scales. If a neuron is sensitive to stimulus spikes that arrive at the expected stimulus rate, and responds with a response rate that is related to the stimulus rate, it temporally integrates. If a neuron is sensitive only to stimulus spikes that arrive in rapid succession, faster than the average stimulus rate, its operational mode has been called coincidence detection. Investigating the level of coincidence detection independently from other neural features is important in understanding neural coding, however, setting up neuron models to spike in a predefined way is not straightforward. We recently proposed a two-dimensional measure that quantifies whether a neuron is doing coincidence detection or integration – a value called the Neural Mode, and that quantifies the amount of excitation or inhibition – a value called the Neural Drive [1]. (Figure 1a shows an overview.) The Neural Mode can be measured easily, but obtaining it analytically is difficult with current neuron models.

In the workshop we would like to propose, explain, and demonstrate a new spiking neuron model – the Difference Neuron – that responds to its stimulus according to a predefined value of the Neural Mode. The amount of integration or coincidence detection is no result of complex property relations, but a parameter of the model.

The neuron uses the Neural Mode and Neural Drive as input space. Simple "Difference Detectors" notice whether stimulus is inside a rectangular receptive field in the Neural Mode and Drive plane. (Figure 1b shows receptive fields.)

We compare the Difference Neuron to a conductance-based leaky Integrate-and-Fire Neuron. While changing from a of sub-threshold to super-threshold regime, the Difference Neuron reproduces the general trend of mean, variance, coincidence detection, and temporal integration of the leaky Integrate-and-Fire Neuron. (Figure 1c shows a sample spike train.)

We investigate the behaviour of sparsely connected networks of Difference Neurons. In two different setups, they show low-response states, oscillatory states, and high activity chaotic states. Using dedicated receptive fields for temporal integration and for coincidence detection, we can influence and measure the values of coincidence detection and integration within a network separately. (Figure 1d shows network activity.)

References

[1] J. Kanev, A. Koutsou, C. Christodoulou, K. Obermayer. Integrator or Coincidence Detector: A Novel Measure based on the Discrete Reverse Correlation to Determine a Neuron's Operational Mode, *Neural Computation*, 28(10):2091-2128, 2016.

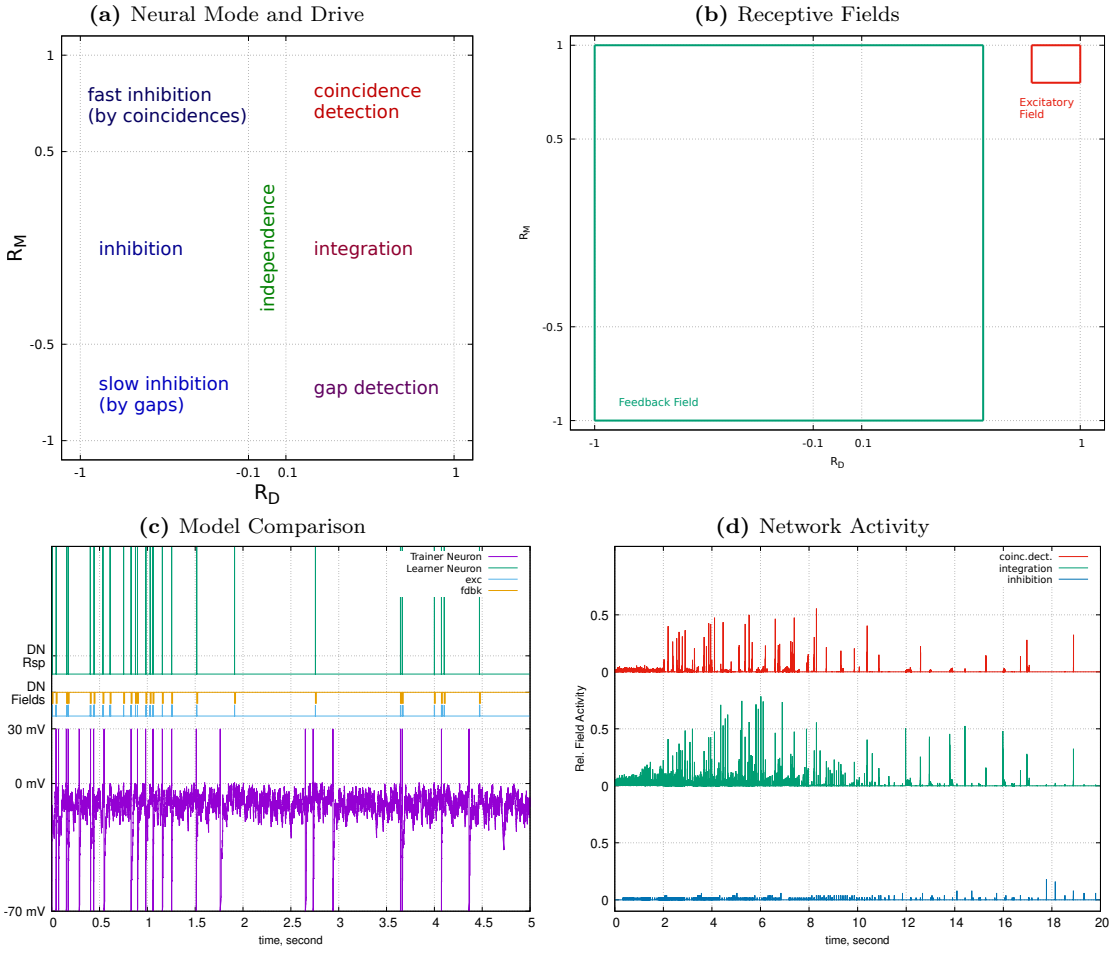

Figure 1: The Difference Neuron

(**a**) The two-dimensional Neural Mode and Drive quantifies a relation between stimulus and response spike trains. The X axis shows the Neural Drive, inhibition on the left (-1), excitation on the right (+1), the Y axis shows the Neural Mode, gap detection at the bottom (-1), integration near 0, coincidence detection at the top (+1). (**b**) Receptive fields within the Neural Mode and Drive plane form a Difference Neuron's input. (**c**) Sample response of a Difference Neuron (top, green, labelled "Learner Neuron"), receptive field activity (middle), and membrane potential of a leaky Integrate-and-Fire neuron (bottom, purple, labelled "Trainer Neuron"), both receiving the same stimulus. (**d**) Amount of coincidence detection, integration, and inhibition in a simulated network of Difference Neurons.

Building stochastic dynamical neural circuits*

Lawrence M. Ward[1] and Priscilla E. Greenwood[2]
(1) Department of Psychology and Djavad Mowafaghian Centre for Brain Health
University of British Columbia, Vancouver, Canada
(2) Department of Mathematics
University of British Columbia, Vancouver, Canada

1 June 2021

The Wilson-Cowan model of a neural mean field is derived from populations of interacting spiking excitatory (E) and inhibitory (I) neurons. A linearization of this and related neural field models around a stable fixed point forms a damped neural circuit that models an elementary perpetual circuit when combined with a small noise. This basic stochastic quasi-oscillator has a remarkable stability property: The difference of the associated E and I phases and the ratio of their envelopes are narrowly distributed around computable constants despite the noise that keeps the oscillator 'alive.' This stability property enables us to build stable stochastic neural structures that share observed properties of a variety of brain areas, including interactions between brain areas, e.g., the cortical-pulvinar system. As an example of how the latter can be accomplished, we analyse the results of a recent paper by Quax et al. [1] and replace their spiking neural network model of cortical populations that receive sine wave alpha-frequency 'pulvinar' input with a stochastic neural field model for both cortical and pulvinar activity.

The linear quasi-cycle oscillators are described in detail in [2] based on a model of [3]:

$$d\mathbb{V} = -\mathbb{A}\mathbb{V}dt + \mathbb{N}d\mathbb{W} \tag{1}$$

where

$$\mathbb{V} = \begin{pmatrix} V_E(t) \\ V_I(t) \end{pmatrix}, \quad \mathbb{A} = \begin{pmatrix} (1 - S_{EE})/\tau_E & S_{EI}/\tau_E \\ -S_{IE}/\tau_I & (1 + S_{II})/\tau_I \end{pmatrix}, \quad \mathbb{N} = \begin{pmatrix} \sigma_E & 0 \\ 0 & \sigma_I \end{pmatrix}, \quad d\mathbb{W} = \begin{pmatrix} dW_E(t) \\ dW_I(t). \end{pmatrix} \tag{2}$$

This model is a description of the time evolution of the local field potentials (LFPs) of two coupled populations of neurons, excitatory, $V_E(t)$, and inhibitory, $V_I(t)$. The parameters in $\mathbb{A}$ represent the synaptic coupling strengths between the excitatory and inhibitory neuron populations, σ_i are the noise strengths, and W_i are standard Wiener noise processes. In previous work (see [4] for a summary) we derived the phase and envelope relationships of the E and I processes [2], showed that Kuramoto-coupled quasi-cycle oscillators behaved similarly to ordinary phase oscillators, displayed the effects of spatially-correlated noise on spatial patterns formed by Mexican-hat-coupled (MHC) populations of quasi-cycle oscillators, demonstrated that spatial phase patterns form with weaker MHC than do amplitude patterns, and showed that amplitudes of MHC populations can be controlled by an adaptive inhibitory mechanism while still permitting spatial patterns in the phases.

*Funded by a grant from NSERC of Canada to LMW.

The paper by Quax et al. [1] describes two separate interacting populations of cortical excitatory (E) and inhibitory (I) Izhikevich spiking neuron models that receive (noisy) alpha-frequency (10 Hz) sine wave input from a putative pulvinar (nucleus of the thalamus) source. The cortical populations generate gamma-frequency (30-50 Hz) oscillations by a PING mechanism in which the E neurons excite the I neurons, which in turn inhibit the E neurons, turning down their own excitation, reducing their inhibition of the E neurons, etc. The two cortical I-neuron populations receive the 10-Hz input with a variable phase delay $\Delta\phi$. Input of 10 Hz sine waves into I populations results in modulation of gamma oscillations at alpha rate in the E populations. Notably, phase coherence between the two alpha-modulated (via I populations connected only to their local E population), one-way feedforward connected, E populations occurs at a specific phase offset ($\Delta\phi \approx -\pi/2$) of the respective two 10 Hz inputs. Consistent with the coherence theory of neural communication [5], signal transmission between the two connected E populations also is most effective at the optimal $\Delta\phi$ for coherence. These effects seem biologically plausible, and are a reasonable model for the effects of attention on perception of visual signals.

We first show, in a Lemma, that the main result of Quax et al., a maximum of E-neuron gamma-frequency phase coherence at a specific value of $\Delta\phi$, arises from a mathematical interaction of alpha- and gamma-frequency sine waves, rather than from specific characteristics of the spiking neuron models. The maximum E-population phase coherence occurs when $\Delta\phi$ matches the phase offset between them. The feedforward connection between the two E-neuron populations is part of the dynamics that causes a phase difference of $\sim -\pi/2$ between them. This is not mentioned by Quax et al. We then substitute EI Equation 1 neural mean field models for the cortical E and I Izhikevich spiking neuron populations in the Quax et al. paper, but still with sinusoidal 10 Hz input to the I processes. In this dimension-reduced formulation, we demonstrate, using simulations, the Quax et al. results pertaining to coherence and signal effects. Finally, we substitute EI Equation 1 neural mean field models for the two, offset, 10 Hz sine waves as well, and again using simulations, we demonstrate the Quax et al. coherence and signal effects using only the quasi-cycle models. Thus, control of cortical gamma phase coherence via alpha phase modulation of the pulvinar can be accomplished in a reduced-dimension, linearized, neural mean field approach.

References

[1] S. Quax, O. Jensen and P. Tiesinga. Top-down control of cortical gamma-band communication via pulvinar induced phase shifts in the alpha rhythm. *PLoS Comput. Biol.*,13(5):e1005519, 2017.

[2] P.E. Greenwood, M.D. McDonnell and L.M. Ward. Dynamics of gamma bursts in local field potentials. *Neural Computa.*, 27:74–103, 2015.

[3] K. Kang, M. Shelley, J.A. Henrie and R. Shapley. LFP spectral peaks in V1 cortex: network resonance and cortico-cortical feedback. *J. Computa. Neurosci.*, 29:495–507, 2010.

[4] C.L. Morrison, P.E. Greenwood and L.M. Ward. Plastic systemic inhibition controls amplitude while allowing phase pattern in a stochastic neural field model. *Phys. Rev. E*, 103:032311, 2021.

[5] P. Fries. Rhythms for cognition: Communication through coherence. *Neuron*, 88:220-235, 2015.

A Mesoscopic Characterization of Sequential Movement related Neuro-motor States in Premotor and Motor Cortices: A Machine Learning Approach

Michael DePass[1], Ali Falaki[2], Stephan Quessy[2], Numa Dancause[2], Ignasi Cos[1,3]

(1) – Universitat de Barcelona

(2) – University of Montreal

(3) Serra-Húnter Research Programme

Movement parameters have been decoded from spikes and local field potentials (LFPs), recorded from the primate motor cortices during movement planning and execution[1,2]. However, the potential of LFPs to provide network-like, distributed characterizations of neural dynamics during the planning and execution of sequential movement tasks remains to be fully understood. Is the aggregate nature of LFPs suitable to construct informative brain state descriptors of movement preparation and execution that characterize the topological and frequential coding of different aspects of behaviour? To investigate this, we developed a computational framework for the analysis of LFPs based on machine learning classifiers and analysed a set of LFP-ensemble neural dynamics from a primate, implanted with several microelectrode arrays in pre-motor and motor cortical areas of both hemispheres. The primate performed a reach and grasp task, consisting of five consecutive states, starting from rest until a rewarding target (food) was attained. We use this five-state task to characterize brain activity and connectivity within eight frequency bands, using electrode power and pair-wise correlations across electrodes as features. Our results show that we could best distinguish all five movement-related states using the highest frequency band (200-500Hz), yielding a 87% accuracy with electrode power, and 60% with pair-wise electrode correlation. The accuracy decreased with frequency band. Further analyses characterized each movement-related brain state, showing differential neuronal population activity at above-gamma frequencies during the various stages of movement preparation and execution. Furthermore, the brain topological distribution for the high-frequency LFPs allowed for a highly significant set of pair-wise correlations, strongly suggesting a concerted distribution of movement planning and execution function is distributed across pre-motor and motor cortices in a specific fashion, and is most significant in the low ripple (100-150Hz), high ripple (150-200Hz) and multi-unit frequency bands. In summary, our results show that the concerted use of novel machine-learning techniques with coarse grained queue broad signals such as LFPs may be successfully used to track and decode fine reach and grasp movement aspects across several brain regions.

References

[1] Bansal AK, Truccolo W, Vargas-Irwin CE, Donoghue JP (2011) Decoding 3D reach and grasp from hybrid signals in motor and premotor cortices: spikes, multiunit activity, and local field potentials. Journal of Neurophysiology 107:1337–1355..

[2] Cisek P, Kalaska JF (2005) Neural Correlates of Reaching Decisions in Dorsal Premotor Cortex: Specification of Multiple Direction Choices and Final Selection of Action. Neuron 45:801–814.

Olfactory neuropils in Amblypygids

Irina Sinakevitch and Wulfila Gronenberg[1]

(1) – Department of Neuroscience,

University of Arizona, Tucson,

AZ 85721

Amblypygids (whip spiders) are nocturnal predators that rely on touch and chemosensation when navigating in the dark. In whip spiders, the first pair of legs is transformed into long sensory organs (antenniform legs) covered with many thousands of mechanosensory, olfactory, and gustatory sensilla, but very little is known about olfactory processing in their central nervous system (*). Here, we neuroanatomically describe the Amblypygid olfactory pathways. Olfactory neurons from the sensilla on the antenniform legs terminate in the first leg neuromere on ca. 460 primary olfactory glomeruli, a very high number for arthropods, suggesting advanced olfactory capabilities. Olfactory projection neurons send their afferents from the olfactory glomeruli to the brain where they terminate on a set of large secondary olfactory glomeruli, located in the mushroom body calyx. The mushroom body calyx also comprises a set of much smaller glomeruli that receive visual input, establishing the multimodal nature of the mushroom body. Both, primary and secondary olfactory glomeruli exhibit a high level of anti-GABA staining, indicating that inhibition plays an essential role in odor processing of amblypygids. In contrast, the small visual mushroom body glomeruli are not modulated by GABA input. Using various neuroanatomical techniques, we describe the amblypygid olfactory circuits and compare them with the olfactory system in other arthropods.

***Sinakevitch I**, Skye M Long, Gronenberg W (2020) The central nervous system of whip spiders (Amblypygi): Large mushroom bodies receive olfactory and visual input. *J Comp Neurol.* 1– 17. https://doi.org/10.1002/cne.25045

The research was supported by NSF grant DEB 1456221 to W.G.

MECHANISMS OF FUNCTIONING OF CONNECTOMES EACH OF WHICH INCLUDES THE NEOCORTEX, HIPPOCAMPUS, BASAL GANGLA, CEREBELLUM AND THALAMUS

Isabella Silkis
Institute of Higher Nervous Activity and Neurophysiology of Russian Academy of Sciences, Moscow, Russia
e-mail: isa-silkis@mail.ru

We suggest possible mechanisms of interdependent functioning of different structures in a connectome that includes the neocortex, hippocampus, basal ganglia, cerebellum and thalamus. These mechanisms are based on previously formulated unitary modification and modulation rules for the efficacy of synaptic transmission between neurons of different types. Using these rules we proposed possible mechanisms of functioning of such parts of a connectome as the hippocampal formation, cerebellum and cortico – basal ganglia – thalamocortical neural loop [1-6]. These mechanisms differ from the generally accepted ones, but the predictions of our models have now received experimental verification. We took into account recent morphological and electrophysiological data on interconnections between mentioned structures that are schematically shown in the Fig. The cerebellum affects the neocortex and basal ganglia through the thalamic nuclei. It also influences the hippocampus through the thalamic nucleus reuniens, retrosplenial and prefrontal cortical areas, medial septum, and supramammillary nucleus. The hippocampus affects the functioning of the cerebellum through the neocortex and pontine nuclei, as well as through the basal ganglia, which output nuclei send GABAergic projections to the subthalamic nucleus and the pedunculopontine nucleus. The basal ganglia, cerebellum, and subthalamic nucleus affect motor activity through the red nucleus. Based on the data on the topographic organization of connections between structures, we proposed that the brain can be considered as a global connectome consisting of separate, similarly organized connectomes. Each of these connectomes includes one neocortical area reciprocally connected with one thalamic nucleus, as well as the corresponding areas of the basal ganglia, subthalamic nucleus, and deep cerebellar nucleus. Dopamine released in response to sensory stimuli and reinforcement modulates the efficacy of synaptic transmission in different structures of a connectome thus determining processing of sensory stimuli of one modality. The mechanisms of signal processing are similar in every connectomes. Therefore, the knowledge of mechanisms of functioning of an individual connectome allows understand mechanisms of functioning of the global connectome that provides the processing of multimodal sensory information, its perception and selection of required reaction. Comparison of the mechanisms of functioning of the connectome in normal and pathological conditions should make it possible to evaluate existing methods of treating neurological diseases and facilitate targeted search for new methods of treatment.
Key words: connectome, neocortex, hippocampus, cerebellum, basal ganglia, synaptic plasticity, dopamine.

1. Silkis I.G. The unitary modification rules for neural networks with excitatory and inhibitory synaptic plasticity. Biosystems,.1998. 48(1-3): 205-213.
2. Silkis I. Interrelated modification of excitatory and inhibitory synapses in three-layer olivary-cerebellar neural network. Biosystems. 2000. 54(): 141-149.
3. Silkis I. The cortico-basal ganglia-thalamocortical circuit with synaptic plasticity. II. Mechanism of synergistic modulation of thalamic activity via the direct and indirect pathways through the basal ganglia. Biosystems. 2001. 59(1): 7–14.

4. Sil'kis I.G. A possible mechanism for the effect of neuromodulators and modifiable inhibition on long-term potentiation and depression of the excitatory inputs to hippocampal principal cells. Neurosci. Behav. Physiol. 2003. 33(6): 529-541.
5. Silkis I. A hypothetical role of cortico-basal ganglia-thalamocortical loops in visual processing. Biosystems. 2007. 89(1-3): 227-235.
6. Silkis I.G. Mechanisms of the interdependent influences of the prefrontal cortex, hippocampus, and amygdala on the functioning of the basal ganglia and the selection of behavior. Neurosci. Behav. Physiol. 2015. 45(7): 729-742.

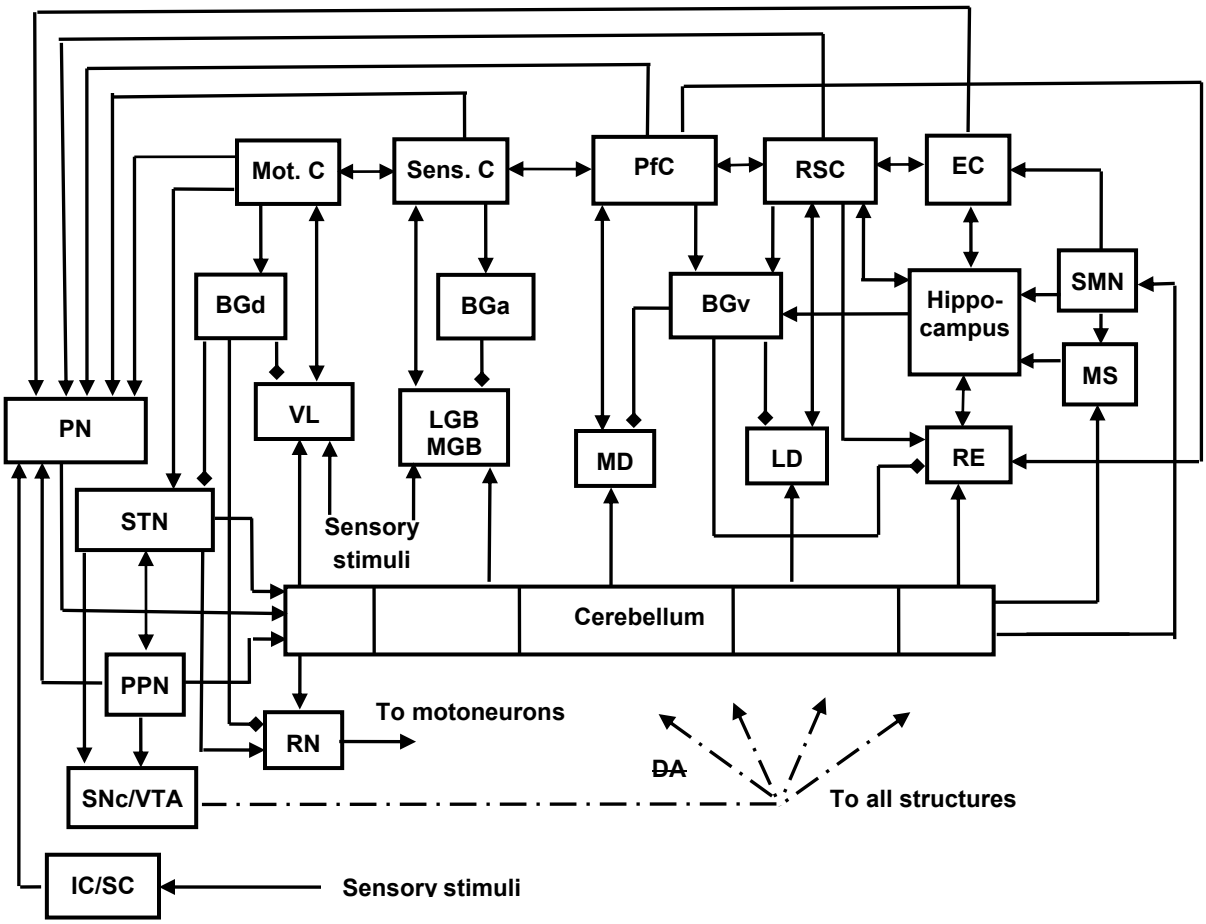

Fig. Topographic organization of neural circuits in the global connectome, consisting of connectomes that are involved in the processing of motor, sensory and limbic information. Each connectome includes a neocortical area reciprocally connected with the thalamic nucleus, as well as the corresponding regions of the cerebellum, basal ganglia, subthalamic nucleus, and pontine nucleus. Cortical areas: Mot. C, motor; Sens. C, sensory; PfC, prefrontal; RSC, retrosplenial; EC, entorhinal. Parts of the basal ganglia: BGd, BGa, BGv, dorsal, associative and ventral, respectively. Thalamic nuclei: VL ventrolateral; LGB, lateral geniculate body; MGB, medial geniculate body; MD, mediodorsal; LD, laterodorsal. SMN, supramammillary nucleus; MS, medial septum; STN, subthalamic nucleus; PPN, pedunculopontine nucleus; PN, pontine nuclei; RN, red nucleus; IC and SC, inferior and superior colliculus, respectively; SNc, substantia nigra pars compacta; VTA, ventral tegmental area; DA, dopamine. Lines ending with arrows and rhombuses, excitatory and inhibitory inputs, respectively.

Phase coupling in interaction networks of neural mass models of cortical columns

Takeshi Abe[1], Yoshiyuki Asai[1] and Alessandro E.P. Villa[2]
(1) AI Systems Medicine Research and Training Center,
Graduate School of Medicine and University Hospital, Yamaguchi University, Japan
(2) Neuroheuristic Research Group, University of Lausanne, Switzerland

Experimental evidence along many years demonstrated the ubiquitous presence of rhythms and oscillatory neural activities at various levels of the mammalian brain. Local field potentials produced by the synchronized activity of large assemblies of neurons propagate through highly dynamic oscillatory waves. A careful balance of excitation and inhibition maintains the neural circuits within proper operational ranges. In this study, we use a neural mass model of cortical columns based on stochastic Jansen-Rit equations to study the functional connectivity within a network of cortical macrocolumns operating in a partially synchronized irregular regime. Here we focus on a heterogeneous topology network, with few nodes acting as hubs while the rest are relatively poorly connected. We aim at presenting a numerical method to infer quadratic phase coupling (QPC) from stationary time series by estimating cross-bicoherence among them in a non-parametric manner. Our results show that our method efficiently detects QPC under various parameter settings, including increasing levels of background noise. We suggest that the neuromodulatory inputs controlling the excitability in cortical columns combined with the local excitatory/inhibitory balance may contribute to set a fine tuning and gating of the information throughout the cortex. Following these results, we discuss the possibility that higher order brain rhythms determined by QPC may represent an important mechanism for the transmission of complex temporal information.

References

[1] Y. Asai and A.E.P. Villa. Integration and transmission of distributed deterministic neural activity in feed-forward networks. *Brain Res.*, 1434: 17–33, 2012

[2] J. Cabessa and A.E.P. Villa. Attractor dynamics of a Boolean model of a brain circuit controlled by multiple parameters. *Chaos*, 28:e106318, 2018.

[3] B. H. Jansen and V. G. Rit. Electroencephalogram and visual evoked potential generation in a mathematical model of coupled cortical columns. *Biol. Cybern.*, 73:357–366 1995.

[4] D. Malagarriga, A.J. Pons and A.E.P. Villa. Complex temporal patterns processing by a neural mass model of a cortical column. *Cogn. Neurodyn.*, 13:379–392, 2019.

Dynamics of brain activity in multisite recordings from behaving parvalbumin deficient mice (PVKO)

A. Lintas[1], R. Sánchez-Campusano[2], A. Gruart[2], J.M. Delgado-García[2] and A.E.P. Villa[1]
(1) Neuroheuristic Research Group, University of Lausanne, Switzerland
(2) Division of Neurosciences, Pablo de Olavide University, Sevilla, Spain

High-frequency oscillations in the ranges of the β- and γ-frequency bands (30-80 Hz) have been suggested to represent a fundamental mechanism of information processing in the forebrain. Almost half of all GABAergic interneurons in the brain express the cytosolic $Ca2^{+}$-binding protein parvalbumin (PV) and recent findings have further demonstrated the key role of hippocampal PV neurons in experience regulated adult learning. PV-deficient mice (PVKO) have been shown to develop highly coherent oscillatory activity. This study reports that PVKO mice present significant deficits in the acquisition of an operant behavioral task, although some individuals may reach a level of performance similar to wild-type mice with a delayed and altered dynamics of learning. We performed multisite recordings of local field potentials (LFPs) and multiple single activity in the basal ganglia-thalamocortical circuit. Our recordings showed that in nucleus accumbens the spectral power at all frequency bands tended to increase in WT and to decrease in PVKO, during the interval when mice moved towards the lever, from the first to the last session. Spectral power of LFPs in β- and γ-frequency bands decreased significantly also in the hippocampus and prefrontal cortex of PVKO compared with WT mice. We observed also a decreased oscillatory activity, as well as less synchronized activity between nucleus accumbens and the prefrontal cortex of PVKO while the mice were freely-roaming. We confirm our previous studies that PV is necessary for a correct signaling during instrumental learning associated with the recognition of natural rewards.

References

[1] A. Gruart, J.M. Delgado-García and A. Lintas. Effect of Parvalbumin Deficiency on Distributed Activity and Interactions in Neural Circuits Activated by Instrumental Learning. *Advances in Cognitive Neurodynamic*, V:111–117, 2016.

[2] A. Lintas A., R. Sánchez-Campusano, A.E.P. Villa, A. Gruart and J.M. Delgado-García. Operant conditioning deficits and modified local field potential activities in parvalbumin-deficient mice. *Scientific Reports*, 11(1):2970, 2021.

[3] B. Schwaller B., I.V. Tetko, P. Tandon, D.C. Silveira, M. Vreugdenhil, T. Henzi, M.-C. Potier, M.R. Celio and A.E.P. Villa. Parvalbumin deficiency affects network properties resulting in increased susceptibility to epileptic seizures. *Molecular and Cellular Neuroscience*, 25:650–663, 2004.

Brain activity associated with personality traits and behavioral strategies revealed by unsupervised analysis of EEG Signal

Qinyue Zheng[1,2], Sihao Liu[3], Alessandro E.P. Villa[1], and Alessandra Lintas[1,4]

(1) NeuroHeuristic Research Group, University of Lausanne, Switzerland

(2) Huazhong University of Science and Technology, Hubei Province, P. R. China

(3) Computer Science Department, University of California, Los Angeles (UCLA), USA

(4) LABEX, HEC-Lausanne, University of Lausanne, Switzerland

In the last decades, the nature of human fairness has been investigated by the Ultimatum Game (UG), a common experimental task in neuroeconomics involving two players. The Proposer is the player who offers how to share an endowment in two parts, and the Responder is the opponent player who can either accept the offer, (and share it accordingly) or to reject it with both players receiving a zero payoff. The recording of brain activity during UG has become one of the most common experimental tasks aimed at studying the decision-making process, being considered to be the most qualifying phase of the expression of will. To better understand what's going on in our brains while we take a decision, here we present an approach aimed at extracting features of brain activity in a completely unsupervised way. Patterns of brain activity can be associated with specific personality trait, assessed by standardaized psychological questionnaires (HEXACO), and behavioral response during an iterated UG (where both players take the role of Proposer and Responder over a long series of runs). Our study revealed different types of fairness tested against willingness-to-share because the players could be clusterized into specify groups characterized by common features in EEG patterns, personality traits and behavior. This approach is likely to open the way to new studies of the neural basis of where and how a "decision" is taken in the brain.

References

[1] Fiori M., Lintas A., Mesrobian S. and Villa A.E.P. Effect of Emotion and Personality on Deviation from Purely Rational Decision-Making. *Studies in Computational Intelligence*, 129–161, 2013.

[2] Guy T.V., Kárný M., Lintas A. and Villa A.E.P. Theoretical Models of Decision-Making in the Ultimatum Game: Fairness vs. Reason. *Advances in Cognitive Neurodynamics*, V:185–191, 2016.

[3] Masulli P., Masulli F., Rovetta S., Lintas A. Fuzzy Clustering for Exploratory Analysis of EEG Event-Related Potentials. *IEEE Transactions on Fuzzy Systems*, 28:28–38, 2020.

A non-monotone bootstrap percolation model of neuronal activity*

Henrik Ekström[1] and Tatyana Turova[1,2]

(1) – Mathematical Center, University of Lund, Sweden

(2) – IMPB - the Branch of Keldysh Institute of Applied Mathematics of Russian Academy of Sciences, Russia.

We consider a model for propagation of electrical impulses, i.e., "activity" in a neuronal network. The neurons are assumed to be placed at the vertices of a square lattice whose edges represent the synaptic connections. Let $\mathcal{G} = (V, E)$ denote the graph induced by the edges of the lattice $\mathbf{Z}^2$ on the set of vertices $V \subseteq \mathbf{Z}^2$. The set of vertices V is partitioned into two subsets $V = V^+ \cup V^-$, corresponding to two types of neurons: excitatory, V^+ and inhibitory, V^-. To keep the empirical ratio 4 between the cardinalities $|V^+|$ and $|V^-|$ we place the inhibitory neurons at the nodes

$$V^- = \{(x, y) : x, y \text{ both even}\}.$$

The state of a neuron $X_v(t)$ at a vertex $v \in V$ at time $t \geq 0$ can either be *active*, which is $X_v(t) = 1$, or *non-active*, which is $X_v(t) = 0$.

Let A_0 be a set of initially active vertices, $A_0 = A_0^+ \cup A_0^-$, where $A_0^\pm \subset V^\pm$. Then, for any $t \geq 0$ given $A_t = A_t^+ \cup A_t^-$ define the active neighbours of a vertex $v \in V$ by

$$N_t^\pm(v) = \{u \in A_t^\pm : (u, v) \in E\}$$

and then set

$$A_{t+1} = \{v \in V : |N_t^+(v)| - |N_t^-(v)| \geq 1\}.$$

Hence, a neuron is active at time $t + 1$ if and only if at time t it has more excitatory active neighbours than inhibitory active ones, no matter its own type. This dynamics of propagation of the initial activity captures features of the "integrate-and-fire" model and is also within a wide class of cellula automata ([1]). Mathematically rigorous theory, however, it is still much limited to the case of monotone dynamics only, i.e., without inbitory units (e.g., [2]).

We suggest a novel approach to analyse the complex behaviour of the model. We first study the trajectories of activation of a single neuron, as independent dynamical systems, and then view a general case as their interaction. This enables us to derive the asymptotic behaviour of the set A_t as $t \to \infty$ depending on the initial activation set A_0. Both the total activation $|A_t|$ as well as the patterns of activity depend in a complex non-monotone way on the size of the initial activation, and moreover are highly sensitive to its configuration.

The marginal cases of (i) sparse and (ii) dense finite initial activation sets $A_0 \subseteq [-k, k]^2$, $k \geq 1$, are studied in detail.

We describe that locally the process of activation on a finite set is periodic and we find its periods.

*This work was partially supported by the Wallenberg AI, Autonomous Systems and Software Program (WASP) funded by the Knut and Alice Wallenberg Foundation.

We provide sufficient conditions for the infinite growth of activation, which in our model can be at most linear. We also find the initial configurations A_0 such that $|A(t)|$ is uniformly bounded for all t.

We show that for some initial configurations of A_0 the set of active cites remains to have a constant size while the location of the active set is moving across the network, constituting a moving front or a wave.

Our results show that the network has a very rich behaviour. It is natural to interpret the limiting cycles as memorized patterns. Furthermore, for some of the limiting patterns we find basins of attraction, i.e., the sets of initial configurations leading to a given dynamical limit, which is an important issue in learning and coding.

References

[1] T. Ceccherini-Silberstein, M. Coornaert *Cellular Automata and Groups*. Springer, 2010. ISBN 978-3-642-14033-4.

[2] B. Bollobás, P. Smith, and A. Uzzell. Monotone cellular automata in a random environment. *Combinatorics, Probability and Computing* , 24(4): Oberwolfach Special Issue Part 1 , July 2015 , pp. 687 - 722.